Kaunas University of Technology

Faculty of Mathematics and Natural Sciences

Dose Planning Risk Estimation for Central Nervous System Cancer Patients

Master's Final Degree Project

Julija Jokšaitė

Project author

Prof. dr. Diana Adlienė

Supervisor

Dr. Evelina Jaselskė, Medical physicist expert

Consultant

Kaunas, 2023

Kaunas University of Technology

Faculty of Mathematics and Natural Sciences

Dose Planning Risk Estimation for Central Nervous System Cancer Patients

Master's Final Degree Project

Medical physics (6213GX001)

Julija Jokšaitė

Project author

Prof. dr. Diana Adlienė

Supervisor

Dr. Evelina Jaselskė, Medical physicist expert

Consultant

Prof. dr. Arvaidas Galdikas

Reviewer

Kaunas, 2023

Kaunas University of Technology

Faculty of Mathematics and Natural Sciences

Julija Jokšaitė

Dose Planning Risk Estimation for Central Nervous System Cancer Patients

Declaration of Academic Integrity

I confirm the following:

1. I have prepared the final degree project independently and honestly without any violations of the copyrights or other rights of others, following the provisions of the Law on Copyrights and Related Rights of the Republic of Lithuania, the Regulations on the Management and Transfer of Intellectual Property of Kaunas University of Technology (hereinafter – University) and the ethical requirements stipulated by the Code of Academic Ethics of the University;

2. All the data and research results provided in the final degree project are correct and obtained legally; none of the parts of this project are plagiarised from any printed or electronic sources; all the quotations and references provided in the text of the final degree project are indicated in the list of references;

3. I have not paid anyone any monetary funds for the final degree project or the parts thereof unless required by the law;

4. I understand that in the case of any discovery of the fact of dishonesty or violation of any rights of others, the academic penalties will be imposed on me under the procedure applied at the University; I will be expelled from the University and my final degree project can be submitted to the Office of the Ombudsperson for Academic Ethics and Procedures in the examination of a possible violation of academic ethics.

Julija Jokšaitė

Confirmed electronically

Julija Jokšaitė. Dose Planning Risk Estimation for Central Nervous System Cancer Patients. Master's Final Degree Project. / supervisor prof. dr. Diana Adlienė; Faculty of Mathematics and Natural Sciences, Kaunas University of Technology.

Study field and area (study field group): Health Sciences, Medical Technologies.

Keywords: central nervous system, organs at risk, planning target volume, CNS cancer, dose planning risk.

Kaunas, 2023. 49 pages.

Summary

While radiation therapy is one of the most commonly implemented treatment methods for central nervous system cancer patients, treatment planning for this location requires great care and accuracy. Exceeding tolerance doses for organs at risk (OARs) due to patient positioning errors can result in short and long-term complications for the patient. Therefore, evaluation of dose planning risk is necessary to improve treatment methodologies and lower the risk of radiation-caused complications.

This work consisted of several parts. First, set-up uncertainties of 64 CNS cancer patients for two radiation therapy treatment units (TRUEBEAM and TRILOGY) were evaluated. Then, planning organ at risk volume (PRV) margins were calculated using two different formulas. Calculated margins varied between 2.51 mm and 2.84 mm. However, due to limitations of the treatment planning system, 3 mm margins had to be used.

In the next part, 27 approved treatment plans with a total prescribed dose of 60 Gy were modified by adding 3 mm PRV margins around the brain stem, chiasma and optic nerves. Modifying plans was necessary to evaluate dose planning risks for selected OARs arising from set-up errors. The evaluation showed that after modification, PRV constraints were exceeded in 55.56 % of plans for the brain stem, in 44.44 % of plans for chiasma, 18.52 % for the left optic nerve and in 22.22 % of plans for the right optic nerve.

All 27 plans were re-planned according to a newly created protocol combining dose constraints for OARs implemented in the clinic and PRV recommendations from the literature. After re-planning, PRV constraints were met for all 27 plans and mean maximum doses were reduced by 3.08 Gy, 2.64 Gy, 2.27 Gy and 1.69 Gy to the brain stem, chiasma, right optic nerve and the left optic nerve, respectively. Implementation of PRV margins reduced dose planning risk without compromising planning target volume (PTV). After re-planning mean PTV coverage decreased by 0.17 %, from 97.83 % down to 97.66 %. No significant changes to the conformity index were observed.

Lastly, after re-planning, the 15 highest-risk treatment plans were additionally investigated by generating uncertainty plans by shifting the isocenter by ±3 mm in x, y and z directions. Analysis revealed that patient set-up uncertainties in the z-direction result in the highest dose planning risk, especially, for chiasma.

Julija Jokšaitė. Dozių planavimo rizikos vertinimas onkologiniams centrinės nervų sistemos vėžio pacientams. Magistro baigiamasis projektas / vadovė prof. dr. Diana Adlienė; Kauno technologijos universitetas, Matematikos ir gamtos mokslų fakultetas.

Studijų kryptis ir sritis (studijų krypčių grupė): Sveikatos mokslai, Medicinos technologijos.

Reikšminiai žodžiai: centrinė nervų sistema, sveikieji audiniai, planavimo taikinio tūris, CNS vėžys, dozių planavimo rizika.

Kaunas, 2023. 49 p.

Santrauka

Nors spindulinė terapija yra vienas dažniausia taikomų centrinės nervų sistemos (CNS) vėžio gydymo būdų, šios lokacijos navikų gydymo planavimas yra sudėtingas ir reikalauja ypač didelio dėmesingumo bei tikslumo. Maksimalios leistinos dozės sveikiems audiniams viršijimas dėl paciento pozicionavimų klaidų gydymo metu gali sukelti tiek trumpalaikes tiek ilgalaikes komplicacijos. Taigi, dozių planavimo rizikos įvertinimas yra itin svarbus spindulinės terapijos gydymo metodikų pagerinimui bei jonizuojančios spinduliuotės sukeltų komplikacijų rizikos sumažinimui.

Atliktas baigiamojo darbo tyrimas susideda iš keletos dalių. Pirmiausia, buvo įvertinti 64 CNS vėžio pacientų pozicionavimo neapibrėžtumai dvejiems linijiniams greitintuvams (TRUEBEAM ir TRILOGY). Tuomet, remiantis dvejomis skirtingomis formulėmis, buvo apskaičiuotos PRV paraštės. Apskaičiuotų paraščių vertės svyravo tarp 2,51 mm ir 2,84 mm (dėl gydymo planavimo sistemos apribojimų, gautos paraštės turėjo būti suapvalintos iki 3 mm).

Kitoje dalyje, 27 patvirtinti 60 Gy suminės dozės gydymo planai buvo modifikuojami įvedant 3 mm paraštes smegenų kamienui, regos nervų kryžmei bei regos nervams. Planų modifikavimas atliktas norint įvertinti dozės planavimo riziką pasirinktoms struktūroms dėl pozicionavimo klaidų. Tyrimas parodė, kad smegenų kamienui PRV dozės buvo viršytos net 55,56 % planų, regos nervų kryžmei – 44,44 % planų, kairiajam ir dešiniajam optiniams nervams – 18,52 % bei 22,22 % planų, atitinkamai.

Visi 27 planai buvo perplanuoti pagal naujai sudarytą protokolą susidedantį iš klinikoje naudojamo planavimo protokolo bei PRV rekomendacijų pateiktų literatūroje. Po perplanavimo, PRV dozių ribos buvo sėkmingai pasiektos visiems pasirinktiems planams. Vidutinė maksimali dozė smegenų kamienui, regos nervų kryžmei, kairiajam bei dešiniajam regos nervams buvo sumažinta per 3,08 Gy, 2,64 Gy, 2,27 Gy ir 1,69 Gy, atitinkamai. PRV pritaikymas sumažino dozės planavimo riziką nepakenkiant planavimo taikinio tūrio (PTV) apsiėmimui. Po perplanavimo, vidutinis PTV apsiėmimas sumažėjo per 0,17 %, nuo 97,83 % iki 97,66 %. Reikšmingų pakitimų konformiškumo indeksui taip pat nebuvo pastebėta.

15 didžiausios rizikos planų po perplanavimo buvo analizuojami papildomai sukuriant neapibrežtumo planus, kurie buvo generuojami paslenkant kiekvieno gydymo plano izocentrą per ±3 mm x, y ir z kryptimis. Neapibrėžtumo planų analizė parodė, kad poslinkiai z kryptimi yra siejami su didžiausia dozės planavimo rizika, ypač, regos nervų kryžmei.

Table of contents

List of Figures

List of Tables

List of Abbreviations

Abbreviations:

CNS – central nervous system

OAR – organ at risk

PRV – planning organ at risk volume

GTV – gross target volume

CTV – clinical target volume

PTV – planning target volume

TV – treated volume

IV – irradiated volume

3D-CRT – 3D-conformal radiation therapy

IMRT – intensity modulated radiation therapy

VMAT – volumetric modulated arc therapy

SRS – stereotactic radiosurgery

SBRT – stereotactic body radiation therapy

IGRT – image-guided radiation therapy

WBRT - whole-brain radiation therapy

MLC – multi-leaf collimator

MU – monitor units

DVH – dose volume histogram

Introduction

According to the statistics, the global incidence of primary central nervous system (CNS) cancers between 1990 and 2019 has increased by 94.35 %; moreover, in 2020 over 300 000 new cases were diagnosed with prognosis indicating a further increase in incidence [1], [2], [3]. CNS cancers for adults include gliomas (glioblastomas, astrocytomas, ependymomas, medulloblastomas, and oligodendrogliomas), hemangioblastomas and rhabdoid tumours. Glioblastomas are the most commonly diagnosed malignant brain tumours. Statistics show that even 48 % of all malignant primary tumours and 57 % of gliomas are glioblastomas [4].

Radiation therapy (RT) is employed to treat CNS cancers by using high-energy radiation to damage the DNA of the cancer cells. Treatment delivery can be performed using advanced RT techniques such as intensity-modulated radiation therapy (IMRT), volumetric modulated arc therapy (VMAT), stereotactic radiosurgery (SRS) and proton therapy [5]. However, even using modern RT techniques, the accuracy of treatment delivery is compromised by uncertainties that arise during treatment preparation and execution [6]. The established practice to reduce the impact of set-up uncertainties on the target coverage is to employ planning target volume (PTV). Doses received by surrounding tissues and organs at risk (OARs) also have to be closely monitored as radiation can cause various short and long-term complications or even permanent damage to these structures [7].

Implementation of a planning organ at risk volume (PRV) has been recommended to account for set-up uncertainties and improve the sparring of OARs. Although the use of PRV has been encouraged in ICRU report 62 and ICRU report 83, detailed guidelines concerning PRV implementation in clinical practice are not provided [8], [9]. Few studies have investigated proposed PRV determination methods in their clinics, however, results are strongly equipment and clinic dependent. Furthermore, in-depth studies on PRV and its influence on the dose planning risks for CNS patients are also very limited. Therefore, it’s important to perform more research and investigate how the use of PRV can affect dose planning risks for CNS cancer patients.

The aim of the work is to assess dose planning risk for CNS cancer patients associated with set-up uncertainties.

Tasks of this work:

1. To calculate patient set-up uncertainties and PRV margins for a selected group of CNS cancer patients.
2. To expand selected organs at risk by calculating PRV margin and re-plan the selected number of plans to evaluate dose planning risks for these structures.
3. To evaluate PRV implementation influence on the PTV coverage and plan quality.
4. To generate uncertainty plans and evaluate directional dose planning risks.

1. Treatment Planning for Central Nervous System Tumours

Radiation treatment planning and delivery is a multi-step process involving numerous medical specialists including radiologists, oncology therapists, radiation therapists and medical physicists. The main purpose of the planning is to prepare a treatment plan which guarantees delivery of the prescribed dose to the target while minimizing the risk of normal tissue irradiation and overdosing. Following sections cover aspects associated with treatment planning for CNS tumours, delivery accuracy, and sparring of critical structures.

1.1. Radiotherapy Planning Volumes

Radiotherapy planning volumes are an essential part of present-day radiation therapy planning. Gross target volume (GTV), clinical target volume (CTV), planning target volume (PTV), treated volume (TV) and irradiated volume (IV) were introduced in ICRU report 50 published in 1993 [10].

GTV encloses the part of the tumour with the greatest tumour cell density, which can be easily observed using clinical imaging techniques or by physically palpating the lesion. Depending on the cancer spread, GTV may be subdivided into primary (GTV-P) tumour, nodal (GTV-N) part involving lymph nodes and metastases (GTV-M). CTV includes GTV and part of the tumour which is not visibly observable, however, still contains tumour cells. While GTV and CTV are clinical concepts, PTV is a geometrical concept used to account for uncertainties that arise during treatment preparation and delivery. The volume enclosed by 95% isodose (or as specified by the oncologist) for treatment is known as the treated volume (TV). Irradiated volume (IV) is the total volume receiving higher than the specified (usually 50% of the total prescribed dose) dose.

Planning organ risk volume (PRV) along with internal target volume (ITV), internal margin (IM) and set-up margin (SM) was presented in ICRU report 62 [8] (Fig. 1). ITV is added around CTV to account for all the changes in the site, shape and size of structures within or near the CTV. According to the proposed definition, PRV is an expansion of OAR with a purpose to account for uncertainties associated with set-up and positional, anatomical changes or motion of the radiosensitive structures.

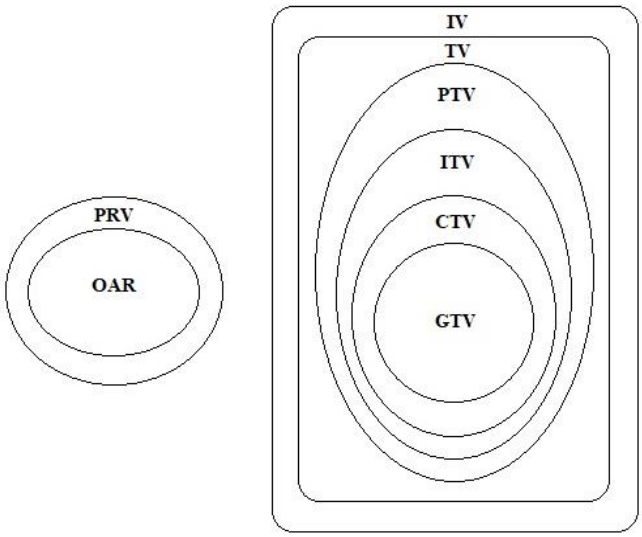

Fig. 1. Radiotherapy Planning Volumes adapted from ICRU report 62 [8]

1.2. Comparison of Radiation Therapy Techniques

Several external beam radiation therapy (EBRT) techniques including 3D-conformal radiation therapy (3D-CRT), intensity modulated radiation therapy (IMRT), volumetric modulated arc therapy (VMAT) and stereotactic radiosurgery (SRS) are available for CNS cancer patients. 3D-CRT is a forward planning technique employing 1-5 fixed geometry photon beams from different directions with uniform intensity. IMRT uses fixed beams as well, however, it employs inverse planning and intensity modulation within each based on optimization objectives. While VMAT makes use of modulated fields and inverse planning, during the treatment delivery its gantry is continuously rotating about the patient table. Small primary brain tumours and metastases of less than 4 cm in diameter are preferably treated with SRS.

In comparison with 3D-CRT, IMRT and VMAT have more complex planning algorithms, require longer dose calculation times, greater number of monitor units (MU) and do not have the possibility to manually select positions of multi-leaf collimator (MLC) leaves. Increased number of MUs results in greater total body exposure which is linked with a higher incidence of secondary malignancies, 1.75% and 1.00% for IMRT and 3D-CRT, respectively [11]. Another comparison between 3D-CRT and IMRT based on irradiated volumes revealed that IMRT can reduce irradiated volumes by 7.5-12.5 %. Although leakage radiation to the periphery is up to 1.9 times greater with IMRT, it offers better sparring of OARs located near the target [12].

According to comparative studies between IMRT and VMAT, the latter is suggested for treating head and neck cancers. VMAT offers a better conformity index, and lower homogeneity index, requires lower MUs and results in lower doses delivered to OARs [13], [14]. Another significant advantage of VMAT is lower delivery times allowing not only to treat a greater number of patients but also lowering the impact of intra-fraction motion [15].

1.3. Radiobiological Effects

Radiation-caused effects can be grouped into acute, subacute and chronic [16]. Acute and subacute effects are considered to be deterministic as they occur within 6 months (acute) or between 6 and 12 months (subacute) after radiation exposure. Deterministic effects have a specific threshold dose and their risk increases with the dose (Fig. 2, a)). To reduce deterministic effects, dose constraints for specific tissues are derived. Chronic or stochastic effects occur after 12 months, there is no threshold dose, however, the severity also increases with dose (Fig. 2, b)).

Known acute radiation-caused effects on the brain include fatigue, loss of hair, loss of hearing, headaches, nausea, drowsiness, temporary demyelination (damage to the myelin sheath) and short-term memory loss. Late irradiation effects are demyelination, vascular abnormalities and necrosis of the white matter. Most of the late symptoms that occur between 6 months and years after radiation therapy are considered irreversible and lead to cognitive deficiency [17], [18]. For patients diagnosed with brain metastases and treated with whole-brain radiation therapy (WBRT), the reported incidence of at least one neurocognitive impairment was 90.5 % [19].

According to various reports, the occurrence of radiation-induced brain necrosis varies from 3% to 24% [20], [21], [22]. Greater doses per fraction and radiation therapy combined with chemotherapy are associated with higher necrosis risk [22]. Radiation necrosis may develop in the location of the tumour, tissues near the tumour site or at the site that received the greatest dose [23].

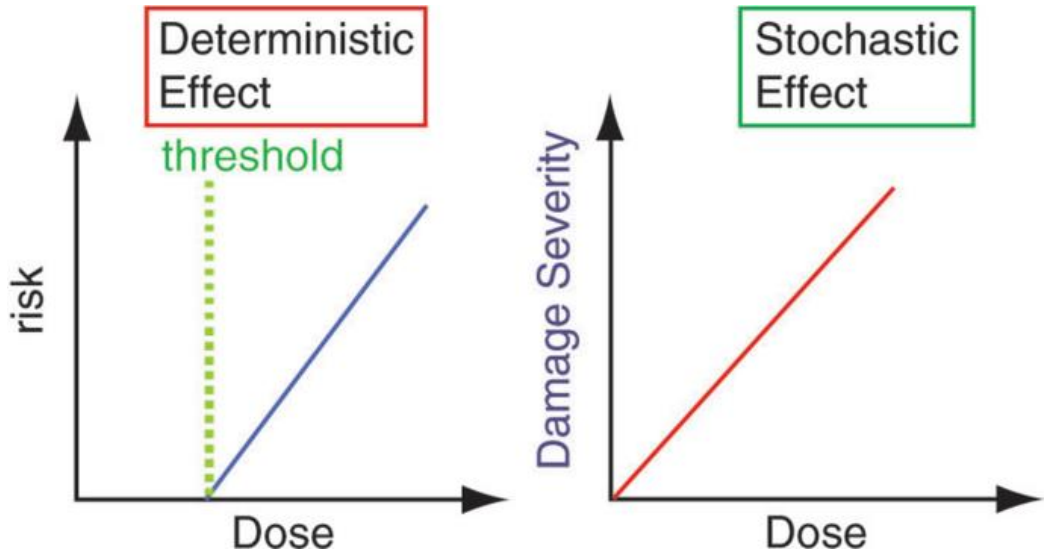

Fig. 2. (a) Deterministic and (b) stochastic effects [16]

1.4. Organs at Risk

Anatomical structures classified as organs at risk in radiation therapy of CNS tumours include the brain, brainstem, chiasm and optic nerves, cornea, lens, retina, cochlea, hippocampus, pituitary and lacrimal glands [24] (Fig. 3). Structures located in the brain are responsible for many important body functions including cognitive functions, motor function, sensory functions and hormonal balance. Radiation-caused damage is associated with symptomatic brain necrosis and higher necrosis susceptibility to the brainstem [26]. Radiation has been reported to cause severe eye dryness [27], perforation of the cornea [28], cataracts [29] and a loss of vision [30]. Irradiation of chiasm and optic nerves is also linked with the development of optic neuropathy [31]. Radiation complications to the cochlea include decrement or loss of hearing [32]. Hippocampus irradiation is associated with memory loss [33], while hypothalamic-pituitary dysfunction has been reported as a result of radiation to the hypothalamus and pituitary gland [34].

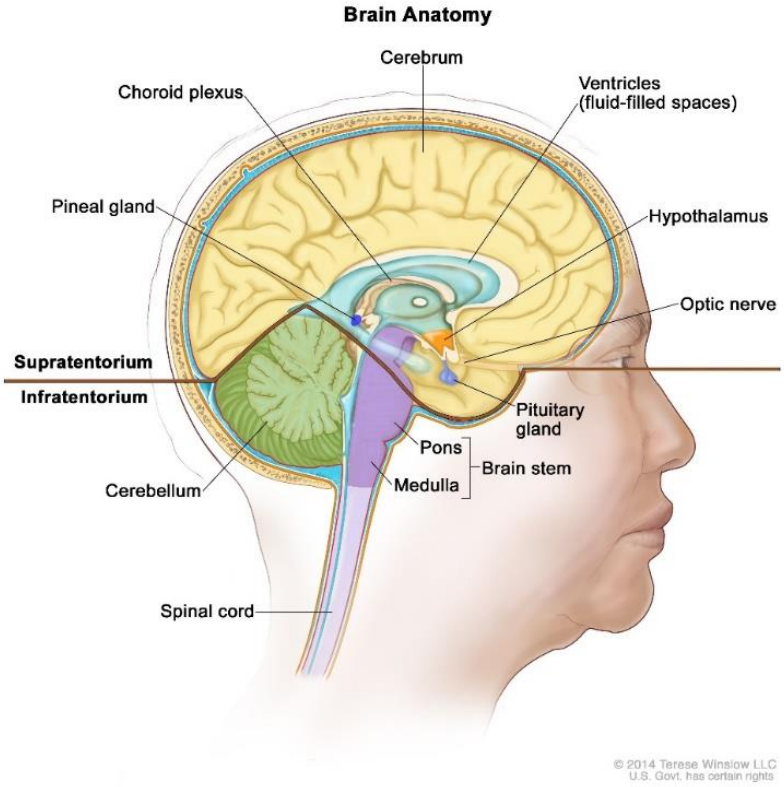

Fig. 3. Anatomical structure of the Central Nervous System [25]

1.5. Dose Constraints

Organs at risk are grouped into serial and parallel [8]. Dose constraints to serial organs such as the brainstem, optic nerves and chiasma, eyes and lenses are based on maximum dose since even a small volume receiving a high dose disrupts organ functioning. Cochlea and lacrimal glands are examples of parallel CNS structures [35], [36]. Small parts of parallel organs receiving high radiation doses do not lead to the disruption of the whole organ function, therefore their dose constraints are based on mean doses or specified volumetric doses.

Dose constraints for various organs at risk are provided by established organizations such as *The European Society for Radiotherapy and Oncology – The Advisory Committee for Radiation Oncology Practice* (ESTRO- ACROP), *The Danish Head and Neck Cancer* (DAHANCA) study group and *The American Association of Physicists in Medicine* (AAPM).

In the guideline for the glioblastoma delineation, ESTRO-ACROP encouraged to always evaluate doses received by the brain, brainstem, optic nerves and chiasma, eyes and lenses, while doses to other structures such as the cochlea, lacrimal glands, hippocampus, hypothalamus and pituitary gland should be assessed depending on the specific clinical situation [37] (table 1).

Table 1. Dose limits to OARs, taken from ESTRO-ACROP guideline [37]

OAR	**Dose constraints, Gy**	**OAR**	**Dose constraints, Gy**
Brainstem	$D_{max} \leq 54$, 1-10 $cm^3 < 59$ (periphery)	Lacrimal glands	$D_{max} < 40$
Chiasm	$D_{max} < 55$	Lens	$D < 6$, $D_{max} < 10$

Cochlea	D_{mean} < 45 (for each)	Optic nerves	$D_{max} \leq 54$
Eyes	Macula < 45	Pituitary gland	D_{max} < 50

In 2020, DAHANCA released updated radiotherapy guidelines for head and neck cancer [38]. For high-importance structures, the guidelines included two different dose constraints – OAR and PRV (table 2). OAR constraint is applied to the organ at risk when its volume is not compromised by the lesion. PRV constraint is the OAR volume with the added PRV margin. The guidelines also present the importance of adherence to the provided constraints grading based on structures. Following dose constraints to the brainstem and spinal cord is considered to be absolute, to optic nerves, chiasm, eyes and lacrimal glands – a must, while dose constraints to the brain, cochlea, and pituitary gland should be followed. The lowest importance is suggested for the hippocampus. According to DAHANCA, the volume receiving the maximum dose should be not greater than 0.027 cm^3 [38].

Table 2. Dose constraints to OAR and PRV provided by DAHANCA [38]

OAR	**Dose constraints, Gy**		**OAR**	**Dose constraints, Gy**	
	OAR	**PRV**		**OAR**	**PRV**
Brainstem	$D_{max} \leq 54$	$D_{max} \leq 60$	Lacrimal glands	$D_{mean} \leq 25$	$D_{mean} \leq 30$
Chiasm	$D_{max} \leq 54$	$D_{max} \leq 60$	Iris, cornea	$D_{max} \leq 30$	$D_{max} \leq 35$
Cochlea	$D_{mean} \leq 45$, $D_{5\%} \leq 55$	$D_{mean} \leq 50$, $D_{5\%} \leq 60$	Optic nerves	$D_{max} \leq 54$	$D_{max} \leq 60$
Eyes	$D_{max} \leq 45$	$D_{max} \leq 50$	Pituitary gland	$D_{mean} \leq 20$	
Brain	D_{1cm3} < 58, $D_{max} \leq 68$		Hippocampus	D40% < 7.2 [EQD2]	

AAPM has published an extensive report on stereotactic body radiation therapy (SBRT). Suggested dose constraints for CNS structures taken from the report are presented in Table 3 [39]. Since SBRT refers to the delivery of radiation treatment in 1-5 fractions with 6-30 Gy doses per single fraction, dose constraints have to be adjusted. For treatment delivered in 5 fractions, the threshold dose received by < 0.5 cm^3 of the brainstem should not exceed 23 Gy, while if the treatment is delivered in a single fraction, < 0.5 cm^3 should not receive more than 10 Gy. Maximum point doses (≤ 0.035 cm^3) to the brainstem in 1 fraction and 5 fraction treatment regimes, should not exceed 15 Gy and 31 Gy, respectively.

Table 3. Dose constraints for the CNS OARs [39]

OAR	**Max volume above the threshold**	**1 fraction**		**3 fractions**		**5 fractions**	
		Threshold dose, Gy	**Max point dose, Gy**	**Threshold dose, Gy**	**Max point dose, Gy**	**Threshold dose, Gy**	**Max point dose, Gy**
Optic pathway	< 0.2 cm^3	8	20	15.3	17.4	23	25
Cochlea	-	-	9	-	17.1	-	25
Brainstem	< 0.5 cm^3	10	15	18	23.1	23	31
Spinal cord	< 0.35 cm^3	10	14	18	21.9	23	30
Medulla	< 1.2 cm^3	7	-	12.3	-	14.5	-

1.6. Set-up Errors

In radiation therapy, different types of errors can impact the accuracy of treatment delivery. Three main types of error sources include organ motion, patient set-up and delineation [40], [41], [42]. Anatomical errors in the brain cavity are relatively small, therefore generally considered not significant. Errors introduced during the delineation process are recommended to be reduced by strictly following delineation guidelines and providing continuous training to radiation oncologists [43]. Set-up errors are separated into systematic and random errors. Systematic positioning errors arise due to the mismatch between the measured patient position before the treatment delivery and the expected positioning in the treatment plan. Systematic errors are assumed to be constant during each radiotherapy treatment session for the patient. Random errors are less predictable and vary between treatment sessions [44].

Random errors result in blurring of the dose distribution (Fig. 4). Dose blurring causes the shift of high isodose lines in the direction of the target, while lines of low isodose shift away from the target. Systematic errors cause dose distribution shifts either towards or away from the organs at risk and are constant for the patient throughout the treatment course [45].

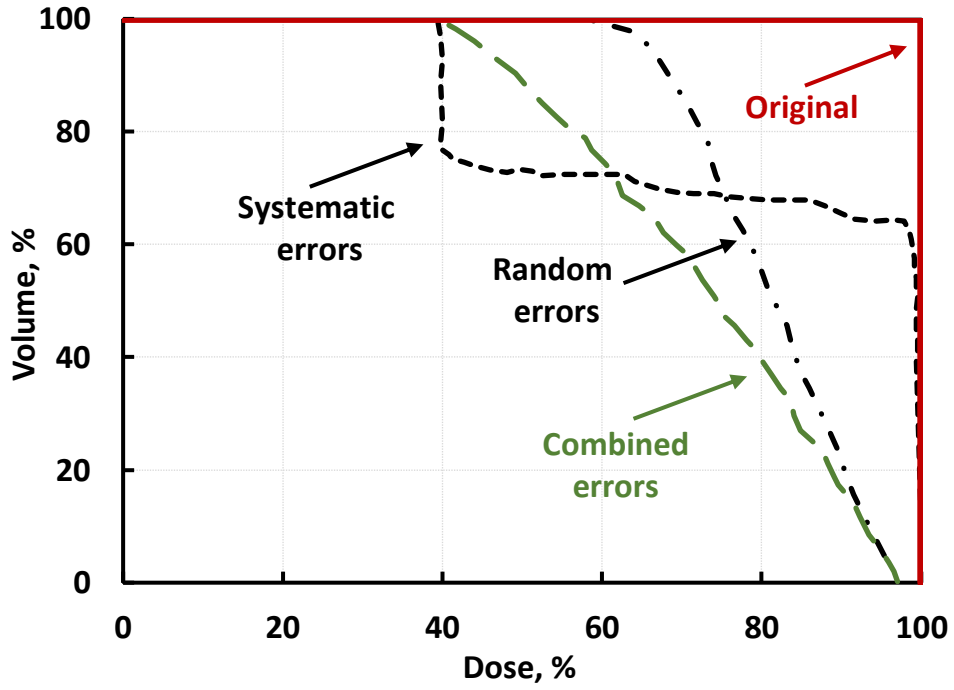

Fig. 4. Schematic illustration of the random and systematic errors effect on the Dose Volume Histogram, adapted from Stroom et al. [45]

1.7. Planning Organ at Risk Volume in Clinical Practice

As reported by the 2020 ESTRO survey [46], a significant number of clinical centres using PRV margins, instead of calculating margins for their radiotherapy treatment units, rely on the historical choices or recommendations provided by multi-institutional studies such as RTOG trials or findings published by smaller groups of researchers. Delishaj et al. investigated set-up errors and proposed a protocol for head and neck cancer treatment with IMRT [47]. Based on the findings, a 3 mm margin expansion was suggested to be added around the brainstem. Out of 360 CBCT scans, greater than 3

mm displacements were observed in 21% of scans after the correction. Therefore, a 3 mm margin around the brainstem and PTV was considered sufficient. While adding a 5 mm margin around the spinal cord was reported as a common practice in an article published in 2004 [48], more recent studies show that due to improvements in the accuracy of treatment delivery techniques, a smaller margin of 3 mm is suggested for the spinal cord. Farace et al. proposed using a 3 mm margin for the spinal cord and a 5 mm margin for the brainstem [49].

While PRV margins are mostly applied to the brain stem and the spinal cord, some studies also recommend using margins around other critical structures. According to RTOG 1205, a minimum of 3 mm PRV margins should be added to optic nerves, and chiasm [50]. Yuan et al. reported using 3 mm PRV margins around the brainstem, bilateral lens and optical chiasm while treating malignant gliomas with IMRT and RapidArc [51]. Some authors also advise adding a 5 mm safety margin around small critical structures such as the cochlea, pituitary gland, arytenoids and chiasm [52].

In recent years, more studies concerning radiation therapy's effect on the hippocampus and neurocognitive deficits have been performed [33]. To preserve memory and neurocognitive functions, RTOG 0933, encourages using a 5 mm margin around the hippocampus [53]. The implementation of the recommended 5 mm margins has been reported in a few other studies [54], [55].

1.8. Planning Organ at Risk Volume Calculation Methods

Research concerning PRV margin calculation methods is limited. Although Monte Carlo (MC) algorithms are the basis of the majority of dose distribution calculation algorithms used in a clinical environment, it requires great computational costs [56], [57]. For this reason, MC is employed to evaluate the viability of other more practical and convenient methods by comparing obtained results with results achieved with MC algorithms. Herschtal et al. used MC simulations to validate their proposed geometrical margin calculation algorithm for hypofractionated radiotherapy [58]. In recent years, MC finds its application in the emerging field of proton-based radiation therapy [59].

The most well-known PRV calculation methods are formulas derived by McKenzie et al. [60] and Stroom et al. [44]. Both formulas have two components: one component represents the standard deviation of systematic uncertainties $\sum$, while the other one – is the standard deviation of random uncertainties σ.

1.8.1. McKenzie's Formula

McKenzie with colleagues worked on the PRV margin determination algorithm, according to which, the dose received by critical organs in 90 % of cases should not exceed set dose constraints for the selected organs [60]. The reasoning behind this approach is analogous to the PTV margin calculation approach proposed by van Herk et al., based on which, in 90 % of the treatment plans, the minimum dose delivered to the CTV is 95 % of the prescribed dose [61].

PRV calculation algorithm suggested by McKenzie et al. consists of several steps. First, the margin covering the mean location of the OAR in 90 % of cases, has to be established using the Gaussian distribution of the OAR positional uncertainty. Then, random and systematic uncertainties have to be evaluated using OAR dose volume histograms. In the next step, an assessment of random uncertainty margins necessity has to be performed. The study explains that in situations where a relatively small part of the OAR enters the high-dose region, due to the random uncertainties, TPS may overestimate

the dose to the organ. Therefore, σ is unnecessary and only systematic uncertainties should be accounted for. For clinical cases when a large OAR is at the edge of the high dose region, due to the random uncertainties, the dose to the OAR slightly increases. However, a small volume of the large or parallel OAR receiving a relatively high dose is tolerable. Therefore, if the OAR is large and parallel, it is advised to use only the margin component associated with systematic uncertainties [60].

Serial and small parallel organs require more consideration when adding margins. In situations where a serial or a small parallel organ is near the high dose region, random uncertainties result in higher doses delivered to these organs than doses calculated by the TPS (Fig. 5). Thus, for serial and small parallel structures, authors suggest to use both margin components [60].

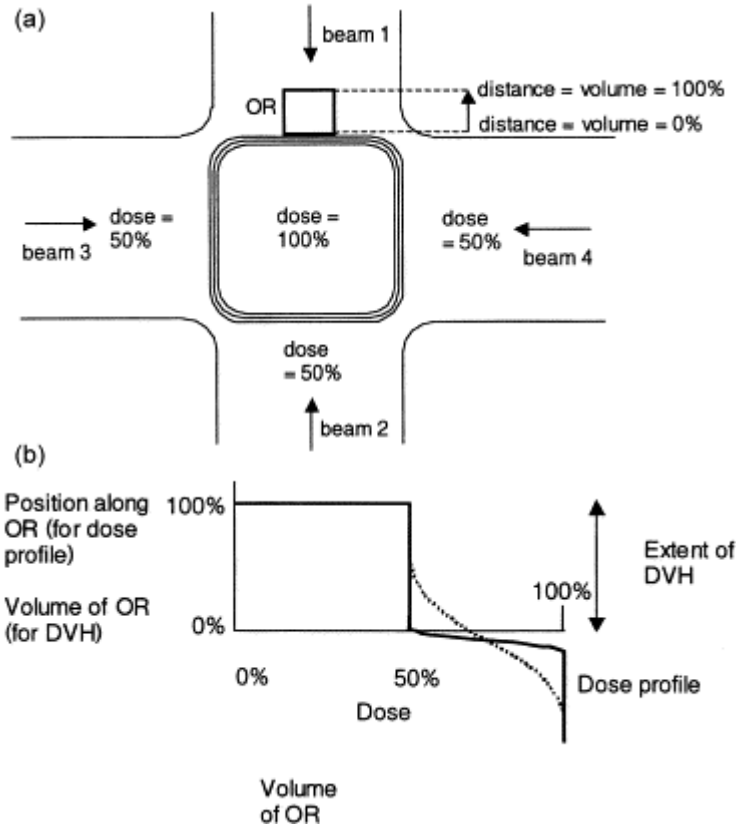

Fig. 5. (a) Schematic illustration of small Organs at Risk near the high dose region; (b) its dose profile with a dotted line representing the effect of uncertainties [60]

In the last step, margins are customized for a particular organ at risk, and the final PRV margin is calculated. Calculations have revealed that to achieve 90% OAR coverage in a chosen direction, a margin of 1.3 ∑ has to be added around the OAR, and to account for the blurring effect caused by random uncertainties proposed margin expansion is 0.5 σ.

Formula from eq. (1) is recommended in one-dimensional cases:

$$\text{PRV margin} = 1.3\Sigma + 0.5\sigma \quad (1)$$

Depending on the anatomical location of the OAR and the PTV, OAR might be surrounded by high-dose regions, not from one direction but from two or three directions as well. Therefore, the margin width should be increased up to 2.2 ∑ or 2.5 ∑ in 2-D and 3-D cases, respectively [60].

1.8.2. Stroom's Formula

In an article published in 2006, Stroom et al. [44] proposed another PRV margin calculation formula based on the investigation of 20 already prepared treatment plans. First, the authors simulated the motion of the spinal cord with standard systematic uncertainties and determined the maximum dose from the mean DVH curve. Obtained DVHs were renormalized for chosen systematic uncertainty concerning the maximum dose constraint of the spinal cord. Then, different margins were added to create PRVs of varying sizes. Using these PRVs' DVH curves, the maximum PRV margin was determined such that the maximum dose constraint would not be exceeded. After repeating the procedure for different systematic and random uncertainties, the margin recipe for systematic and random uncertainties was observed to follow the ratio margin/$\sum$ and margin/σ, respectively.

After evaluation of obtained margins for each plan, the average margin recipe was found:

$$\text{PRV margin} = 1.6\Sigma + 0.2\sigma \quad (2)$$

The authors argue that the PRV concept is useful only for serial organs such as the spinal cord, where dose constraints are based on maximum dose, and stress the need for other ways to be developed to include geometric uncertainties of OARs in radiotherapy planning [44].

1.8.3. Comparison of Calculation Formulas

A comparison of PRV calculation using McKenzie et al. and Stroom et al. formulas is presented in Table 4.

Table 4. Summary of formula-based PRV margin calculation methods

Literature source	**Margin calculation formula**	**RT method**	**Structures**	**Recommended margins, mm**		
				Lateral	**Vertical**	**Longitudinal**
Li et al. [61]	McKenzie et al.	IMRT	Brainstem Spinal Cord Chiasm Eyes Lens Optic Nerves Inner Ears	0.08 0.91 0.43 0.4 1.54 0.89 0.24	0.3 1.34 0.1 0.87 1.85 1.14 0.8	0.05 0.59 0.24 0.29 0.35 0.5 0.15
Breen et al. [62]	McKenzie et al.	IMRT	Spinal Cord	5.4		
Piotrowski et al. [63]	McKenzie et al.	HT	Lens	1.9	1.8	1.3
Fourati et al. [64]	McKenzie et al.	IMRT	Brainstem	2.0		
Zhang et al. [65]	McKenzie et al.	IMRT	*N/A*	1.5	1.7	1.7
Suzuki et al. [66]	McKenzie et al.	IMRT	Mandible Maxilla Cervical Vertebrae	1.8 2.0 2.2	1.7 1.6 2.2	2.4 2.1 2.4
Mongioj et al.[67]	McKenzie et al.	IMRT	Brainstem Spinal Cord	2.3 2.0	2.1 3.8	3.5 3.2
Koivumäki et al. [68]	McKenzie et al.	VMAT	Heart	3.0	5.0	4.0

Park et al. [69]	Stroom et al.	3D-CRT, IMRT	Spinal Cord	5.6	1.8	-
Chang et al. [70]	Stroom et al.	IMRT	Spinal Cord* Spinal Cord**	0.75 1.22	0.84 0.94	0.67 0.79
Laaksomaa et al. [71]	Stroom et al.	IMRT	Heart Shoulder	- 3.0	- 6.0	7.0 -

* Single metastases;
** Multiple metastases.

Since its derivation in 2002, the implementation of the PRV margin calculation formula (eq.1) has been reported in numerous studies. PRV formula was successfully applied in a study aiming to estimate geometrical changes in CNS organs at risk for patients treated with radiation therapy and chemotherapy [61]. Suzuki et al. analysed intrafractional organ motion and interfractional set-up errors and applied McKenzie's formula to evaluate appropriate PRV margins for head and neck cancer patients [66]. Li et al. investigated PRV margin expansion for different segments of the spinal cord using IGRT CT and non-IGRT CT images [72].

Breen et al. [62] used the McKenzie et al. formula to evaluate PRV margins of the spinal cord for oropharyngeal cancer patients by simulating the impact of set-up uncertainties to assess the probability of the spinal cord receiving a particular dose. Simulation of systematic and random uncertainties defined by 3-D Gaussian distribution with 3 mm standard deviation in every direction was simulated separately. Using McKenzie et al. formula, 6 mm PRV a margin for the spinal cord was obtained. The study found that the probability of the spinal cord with a 6 mm PRV margin receiving a 45 Gy dose is less than 1 % [62].

One study reported using Stroom's formula to calculate the margin around the spinal cord for 11 head and neck cancer patients [69]. In another study, Stroom's formula was used to calculate the spinal cord margin for Vertebral Metastases patients treated with stereotactic body radiotherapy [70]. The study found that PRV margins for single vertebral metastases varied between 0.67 mm and 0.84 mm, while for multiple vertebral metastases slightly greater margins were obtained, between 0.79 mm and 1.22 mm. Therefore, the authors concluded that using 1.5 mm margins for the spinal cord in their clinical centre is appropriate.

2. Methodology

2.1. Patient Selection

64 patients diagnosed with CNS cancer and treated using radiation therapy were randomly selected for the research project. Pediatric patients were excluded from the project. All patients were treated with 6 MV energy using the VMAT treatment delivery technique. The majority of patients were between 36 and 75 years old during the treatment (Fig. 6, a)). The total prescribed dose for 35 out of 64 patients was 60 Gy (Fig. 6, b)), which is the standard treatment dose for CNS tumours. Lower prescribed doses were used to carry out palliative treatment, to treat recurrent tumours or to spare critical structures that significantly overlap with the target. 48 patients were treated using standard fractionation of 2 Gy, other types of fractionation were applied depending on the clinical case (Fig. 6, c)).

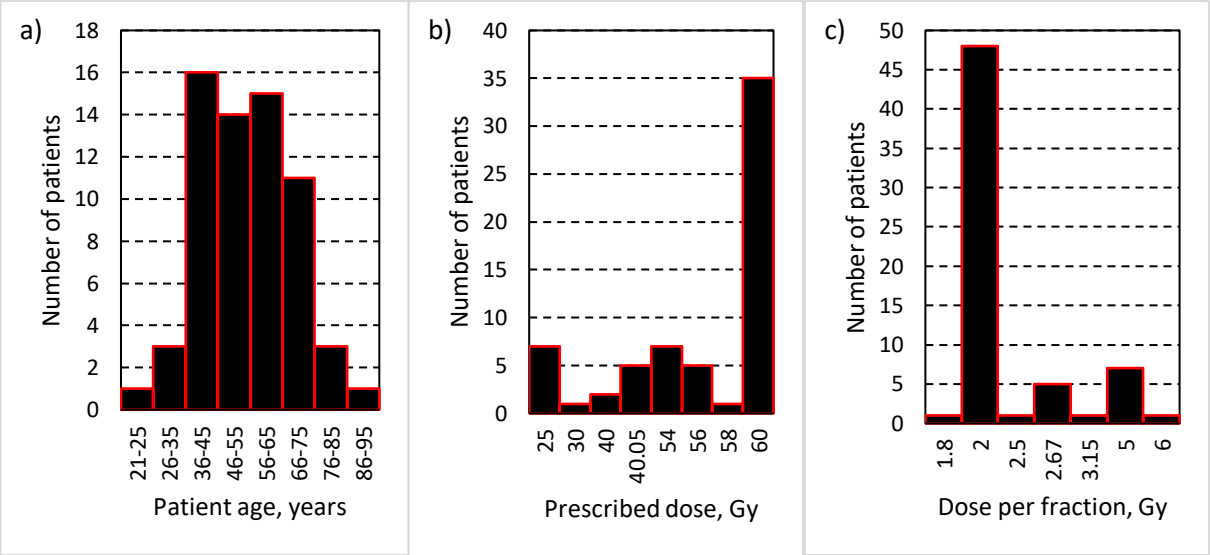

Fig. 6. Statistics of the 64 patients: (a) patient age; (b) total prescribed dose and (c) dose per fraction

2.2. Calculation of Set-up Uncertainties and Planning Organ at Risk Volume

Out of 64 patients, only the patients that completed the treatment and underwent position verification with cone-beam computed tomography (CBCT) before the delivery of each fraction were included in the calculation of set-up uncertainties. Initial patient images were retrieved with LightSpeed RT 16 CT simulator. The width of each slice was 0.25 cm, and images were reconstructed from 512×512 pixel matrice. Before each treatment procedure, CBCT images were obtained with the on-board imager (OBI) system integrated into the linear accelerator as a part of the IGRT daily position verification protocol.

Out of 43 CNS cancer patients that met the requirements, 8 patients were treated with TRILOGY linear accelerator and 35 patients with TRUEBEAM linear accelerator. TRUEBEAM has smaller MLC leaves allowing to deliver treatment with greater accuracy, which is especially important in the head region, therefore, most radical CNS cancer patients are treated with this treatment unit.

Displacements in vertical, longitudinal and lateral directions were extracted from the offline review for each patient from the CBCT scans that were performed before the delivery of each fraction (Fig.

7). In total, displacements from 167 and 992 CBCT scans were analysed for TRILOGY and TRUEBEAM, respectively.

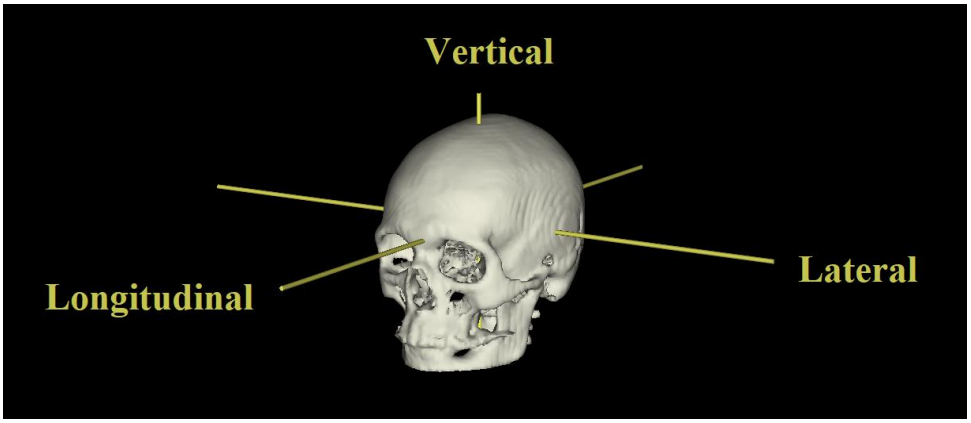

Fig. 7. Directions along which the set-up uncertainties were measured in relation to the anatomical position of a patient

Systematic and random uncertainties were calculated according to the methodology proposed by van Herk [73] (table 5):

1) Mean and standard deviation of each patient positioning were calculated;
2) Systematic uncertainties were obtained by calculating the standard deviation of the mean from step 1.
3) Random uncertainties were calculated by taking the root mean square of the standard deviation from step 1.

RStudio software was used to perform the calculations.

Table 5. Calculation example of mean, systematic and random uncertainties for four patients using set-up uncertainties

Fraction no.	**Displacements in the vertical direction, mm**				
	Patient 1	**Patient 2**	**Patient 3**	**Patient 4**	
1	-0.26	-0.21	0.05	0.32	
2	-0.16	-0.26	-0.08	0.23	
3	-0.12	-0.29	0.03	0.34	
4	-0.24	-0.23	0.16	0.44	
Mean	-1.95	-2.48	0.40	3.33	$\sum = 2.65$
SD	0.66	0.35	0.98	0.86	$\sigma = 0.75$

PRV margins were calculated using the formulas proposed by McKenzie et al. (eq. 1) and Stroom et al. (eq. 2).

2.3. Planning Organ at Risk Volume Expansion for Organs at Risk

Since the number of patients treated with TRILOGY was limited, plan modifications were performed only with treatment plans delivered using TRUEBEAM. In total, 27 CNS cancer patients treated with

60 Gy delivered in 30 fractions (2 Gy/fr) were included in the modification of the original treatment plan by adding PRV margins.

Three serial OARs (brain stem, chiasma and optic nerves) were the selected structures for the addition of PRV margins. Volumes of these structures were expanded by a 3 mm margin in all directions (Fig. 8). Doses delivered to PRVs were evaluated based on dose constraints implemented in the clinic and PRV dose constraints provided by DAHANCA.

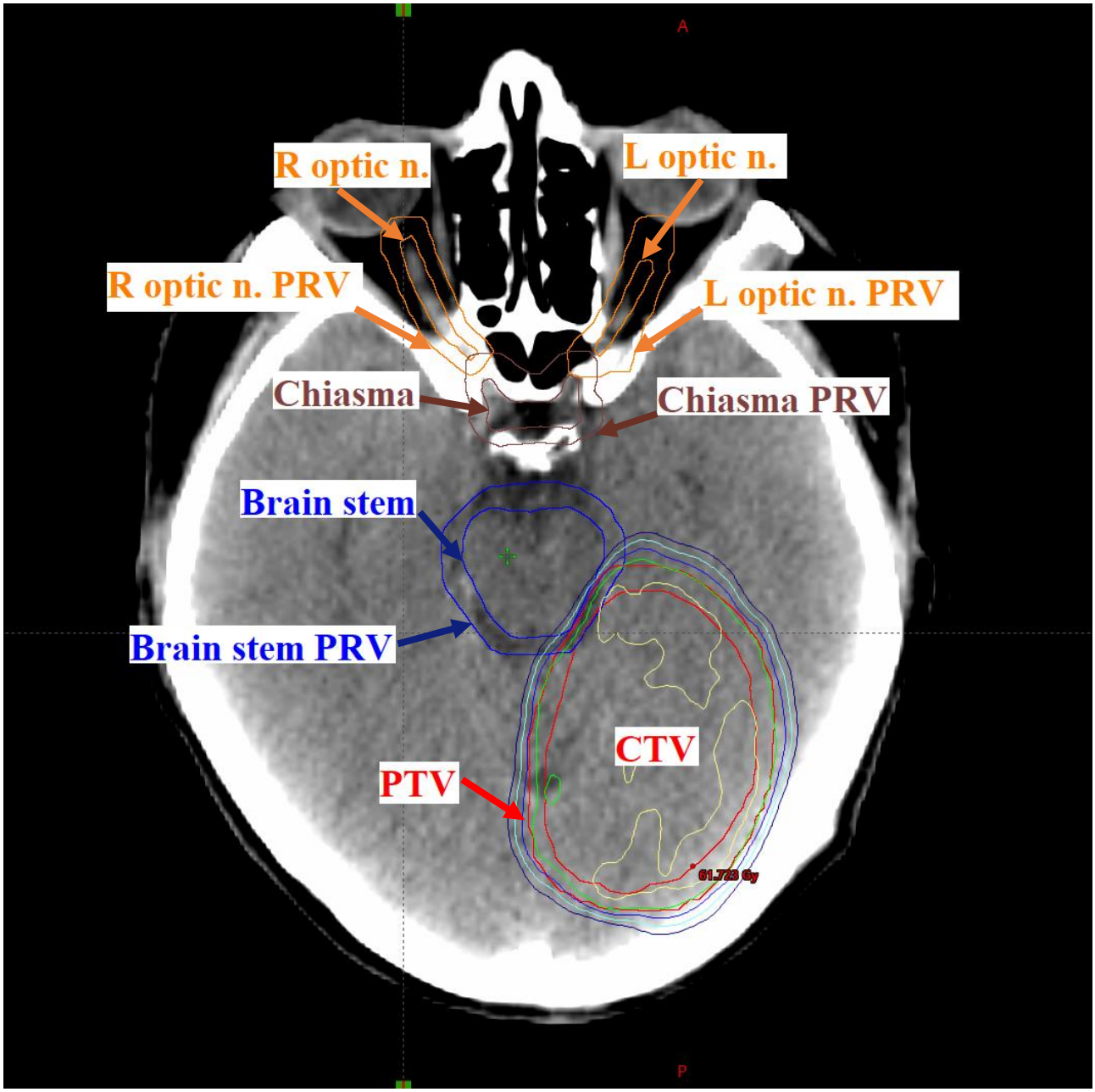

Fig. 8. Brainstem, right optic nerve, left optic nerve and chiasma expanded by 3 mm PRV margin; PTV and CTV structures marked in red

2.4. Re-planning Protocol

After the addition of a 3 mm PRV margin around the selected OARs, 27 approved treatment plans were re-planned using Varian Eclipse 16.1 AAA algorithm. The re-planning aimed to create new plans with additional PRV structures based on the original treatment plans reaching all dose

constraints and maintaining appropriate plan quality. New clinical goals protocol was created combining dose constraints for OARs implemented in the clinic and dose constraints for PRVs recommended by DAHANCA (Table 6.).

To investigate dose planning risks and random uncertainties associated with insufficient experience of a planner, all the plans were re-planned maintaining the same geometry as the original treatment plans.

Optimization was performed with Model PO_16.1: photon optimizer. The convergence mode of the optimized was set to on and the aperture shape controller was set to very high. During the optimization, PTV priority was around 110, while the priority of all the other structures initially was set to 50 and increased by 10-20 if needed. After the optimization, plans were normalized to the target mean. If normalization to the mean was not viable, the plan was normalized to reach PTV coverage requirements.

Newly calculated treatment plans were compared to the original plans based on PTV coverage and doses received by the brainstem, chiasma and optic nerves.

Table 6. Clinical goals protocol

No.	Structure	Objective	Variation
Most important			
1	PTV	V 95 % ≥ 95 %	
Very important			
2	CNS-PTV	V 60 Gy ≤ 3.00 cm^3	
2	Brain stem	V 59 Gy < 10 cm^3	
4	Brain stem surface	D_{max} ≤ 60 Gy	
5	Brain stem interior	D_{max} ≤ 54 Gy	
6	Chiasma	D_{max} ≤ 55 Gy	
7	Left optic nerve	D_{max} ≤ 55 Gy	
8	Right optic nerve	D_{max} ≤ 55 Gy	
Important			
9	Pituitary	D_{mean} ≤ 20 Gy	≤ 40 Gy
10	Left lens	D_{max} ≤ 10 Gy	
11	Right lens	D_{max} ≤ 10 Gy	
12	Hippocampus	D 40 % ≤ 7.30 Gy	
13	Left cochlea	D_{mean} ≤ 32 Gy	≤ 45 Gy
14	Right cochlea	D_{mean} ≤ 32 Gy	≤ 45 Gy
PRV			
15	PRV brain stem	D_{max} ≤ 60 Gy	
16	PRV chiasma	D_{max} ≤ 60 Gy	
17	PRV left optic nerve	D_{max} ≤ 60 Gy	
18	PRV right optic nerve	D_{max} ≤ 60 Gy	

2.5. Generation of Uncertainty Plans

After the addition of PRV margins to the original treatment plans, 15 out of 27 plans did not pass the set dose constraints. Therefore, after re-planning, these high-risk plans were evaluated further by simulating patient set-up errors by shifting isocenter ± 3 mm in longitudinal, lateral and vertical directions (Fig. 9).

Uncertainty plans were generated to evaluate, if treatment plans created using PRV are able to reduce dose planning risks and meet dose constraints when 3 mm patient set-up errors are present.

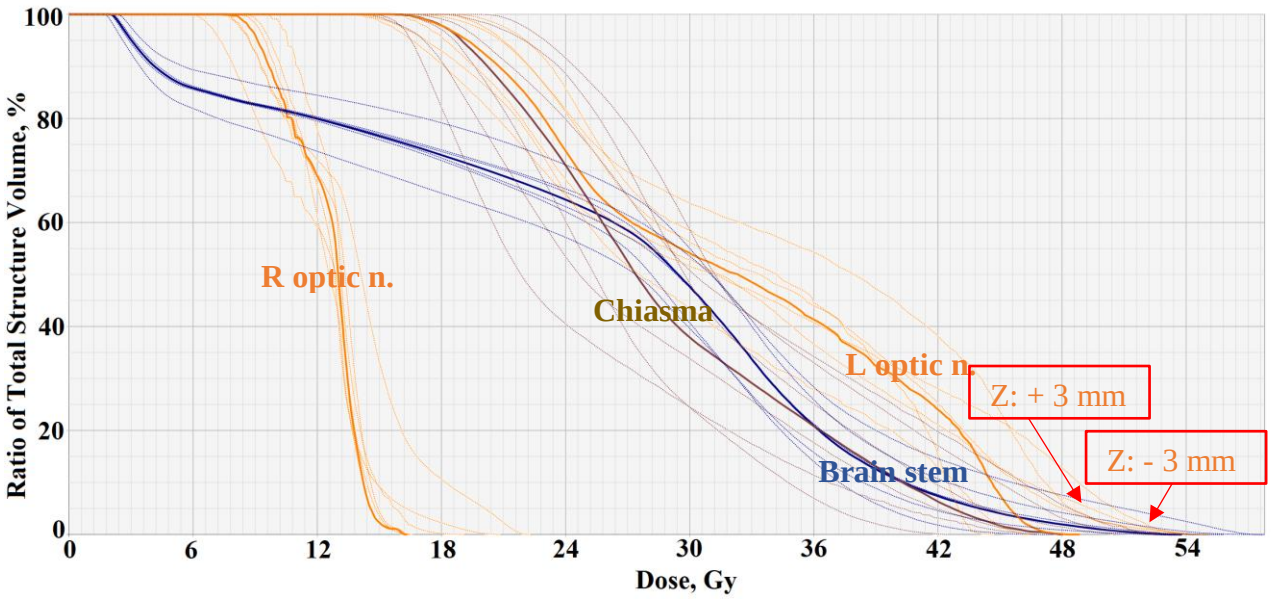

Fig. 9. Dose volume histogram of an uncertainty plan; DVH lines of uncertainty plans exceeding tolerance doses are marked with red arrows

3. Results and discussion

3.1. Evaluation of Set-up Uncertainties and Planning Organ at Risk Volume Margins

The main parameters of uncertainties for TRUEBEAM (TB) and TRILOGY are presented in Table 7. For both treatment units, the greatest mean set-up uncertainties of -1.88 mm (TB) and 2.06 mm (Trilogy) were observed in the vertical direction. Mean set-up uncertainty in the longitudinal direction for TB was two times lower than for TRILOGY, 0.51 mm and 1.10 mm, respectively. For both units, the lowest mean was observed in the lateral direction, 0.27 mm for TB and 0.39 mm for Trilogy.

A study investigating set-up uncertainties for different anatomic locations also found that for the brain the smallest mean of 0.26 mm was in the lateral direction, while for longitudinal and vertical directions, mean set-up uncertainties were 0.47 mm and 0.42 mm, respectively [74].

For TB systematic uncertainties in all directions were greater than random and varied between 1.43 mm and 1.56 mm. For Trilogy, systematic uncertainties in vertical and longitudinal directions also were greater than random uncertainties, while in lateral direction systematic and random uncertainties were 0.75 mm and 1.00 mm, respectively. Another study evaluating set-up uncertainties for CNS patients has reported systematic uncertainties between 1.21 mm and 1.89 mm, and significantly lower random uncertainties (0.18 - 0.27 mm) [75].

Oh et al. performed analysis on set-up uncertainties and reported mean systematic uncertainties of -2.47 mm, 0.48 mm and -0.19 mm in the vertical, longitudinal and lateral directions, respectively. Mean values of random uncertainties were more uniform, 1.06 mm, 1.43 mm and 1.01 mm in the respective directions. [76].

Table 7. Calculated values of mean, systematic (∑) and random (σ) set-up uncertainties

Parameter	TRUEBEAM			TRILOGY		
	Vertical, mm	Longitudinal, mm	Lateral, mm	Vertical, mm	Longitudinal, mm	Lateral, mm
Mean set-up uncertainty	-1.88	0.51	0.27	2.06	1.10	0.39
∑	1.43	1.50	1.56	1.40	1.63	0.75
σ	1.30	1.15	1.10	1.20	1.14	1.00

Set-up uncertainties for TB were based on 992 CBCT measurements, while for Trilogy, due to the limited number of patients, the number of CBCT measurements was only 167. For this reason, further analysis was performed only with TB measurements.

The normality of the set-up uncertainties was evaluated using density histograms and Q-Q plots (Fig. 10-11). For the most part, uncertainties in all directions laid on a straight line. For positive values, set-up uncertainties in vertical and longitudinal directions deviated from the straight line considerably, while the deviation of set-up uncertainties in the lateral direction from the straight line was less significant. However, according to the Shapiro-Wilko test, these distributions cannot be considered normal as the p-value in vertical, longitudinal and lateral directions was 9.939×10^{-14}, 1.416×10^{-8} and 7.197×10^{-5}, respectively. Although formulas for safety margins are derived under the assumption that uncertainty distributions are normal, in practice set-up uncertainties do not follow standard normal distribution [77].

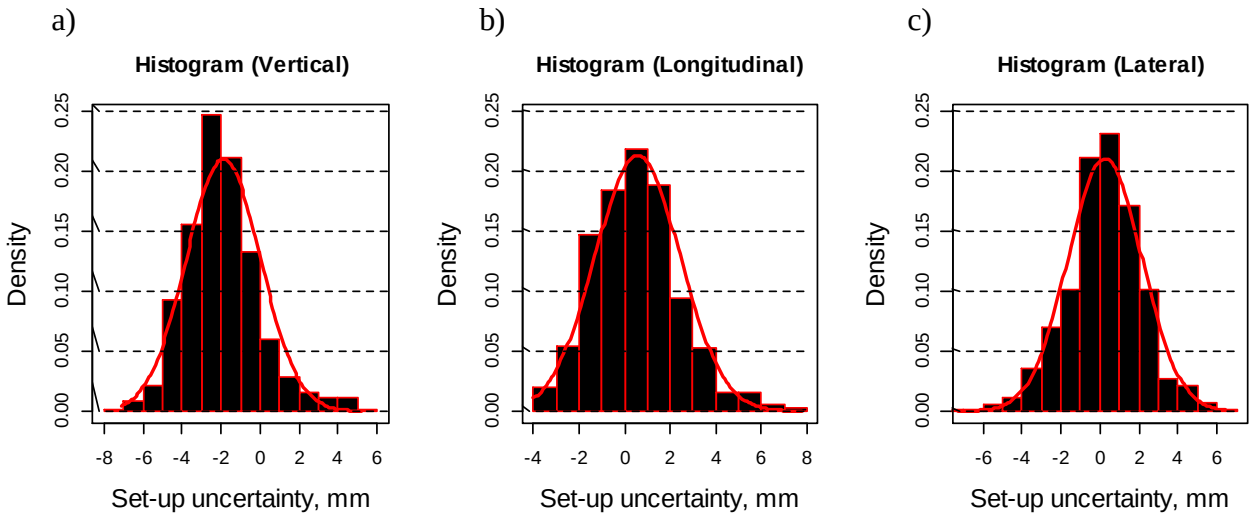

Fig. 10. Density histograms of set-up uncertainties in (a) vertical, (b) longitudinal and (c) lateral directions

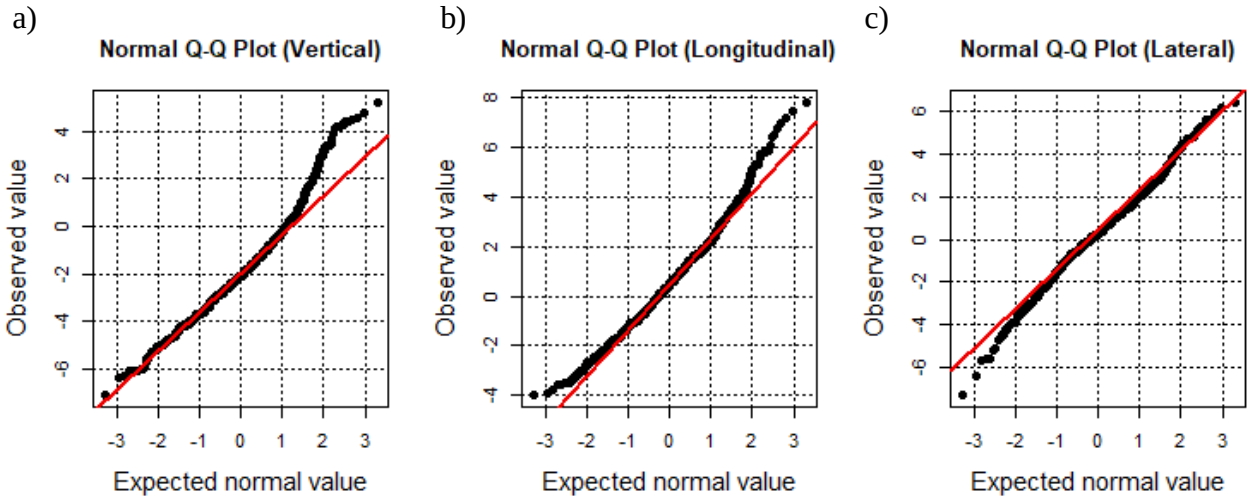

Fig. 11. Q-Q plots of set-up uncertainties in (a) vertical, (b) longitudinal and (c) lateral directions

PRV margins for TRUEBEAM and Trilogy treatment units in different directions calculated using two formulas are presented in Table 8. For TB, based on McKenzie's formula, margins in all the directions were relatively even, between 2.51 mm and 2.58 mm. Using Stroom's formula, variation was slightly greater, between 2.54 mm and 2.72 mm. For TB, the smallest margins were obtained in the vertical direction, while the greatest – in the lateral. A different tendency was observed for Trilogy with the greatest margins observed in the longitudinal direction and the smallest in the lateral. According to different studies, PRV margins can vary between 0.08 - 3.8 mm [61], [64], [65], [67]. Therefore, values of PRV margins obtained from measurements in the clinic are in accordance with results obtained in other radiotherapy clinics.

For TRUEBEAM maximum PRV margin was 2.58 mm and 2.72 mm using McKenzie's and Stroom's formulas, respectively (table 8). However, since the treatment planning system allows only integer numbers for margins in millimetres, the value of the PRV margin was rounded up to 3 mm.

Table 8. Calculated PRV margins

Formula	TRUEBEAM			TRILOGY		
	Vertical, mm	Longitudinal, mm	Lateral, mm	Vertical, mm	Longitudinal, mm	Lateral, mm
McKenzie et al. [60]	2.51	2.53	2.58	2.42	2.70	1.47
Stroom et al. [44]	2.54	2.63	2.72	2.48	2.84	1.39

3.2. Evaluation of Planning Organ at Risk Volume Doses

Expansion of OARs by 3 mm led to a significant increase in maximum doses delivered to the structures. The mean maximum dose to brainstem increased by 5.87 Gy (± 4.83 Gy), to chiasma by 6.37 Gy (± 4.56 Gy), to the left optic nerve by 4.57 Gy (± 4.30 Gy) and to the right optic nerve by 6.08 Gy (± 6.39 Gy) (Fig. 12). Large standard deviation of the mean doses shows significant variation in the maximum doses for different patients.

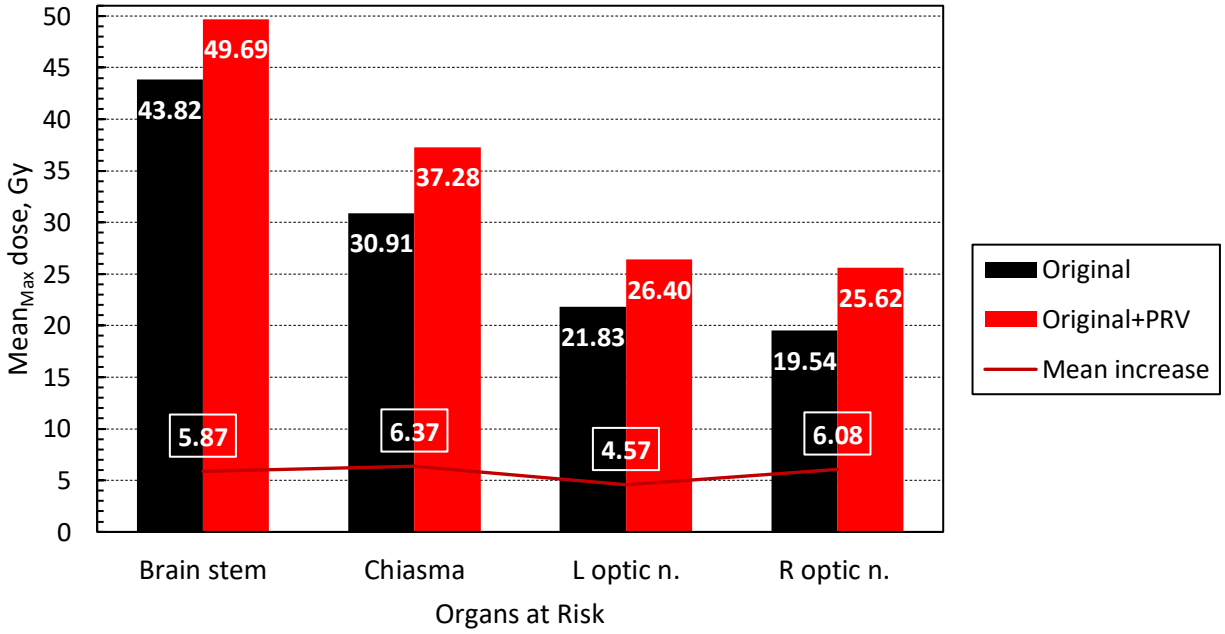

Fig. 12. Mean maximum doses received by different structures in original plans and after adding PRV

As the brain stem is located in the centre of the brain, any large tumour is significantly closer to the brain stem resulting in a higher maximum dose. Optic nerves received considerably lower maximum doses since the tumour has to be in a more specific location to affect the dose delivered to these structures.

First, doses received by expanded structures were evaluated with respect to the protocol implemented in the clinic, according to which, the maximum dose to the brainstem should not exceed 60 Gy, while tolerance doses for optic nerves and chiasma are 55 Gy (Fig. 13). For the brainstem, dose constraints were not met in 55.56 % of plans. A study investigating radiation-induced necrosis of the brain stem found that when 1 cm^3 of the brain stem receives a higher than 60 Gy dose, the risk of necrosis is 15.7 % [78]. Chiasma received more than 55 Gy in 44.44 % of plans and dose constraints to the left and right optic nerves were exceeded in 18.52 % and 22.22 % of plans, respectively. Therefore, in

the presence of patient positioning errors, the risk for the brain stem to receive higher than tolerance dose, is very high. For chiasma and optic nerves, the risk is lower, however, still, significant as maximum radiation doses between 55-60 Gy are are associated with 3 % to 7 % toxicity risks [79].

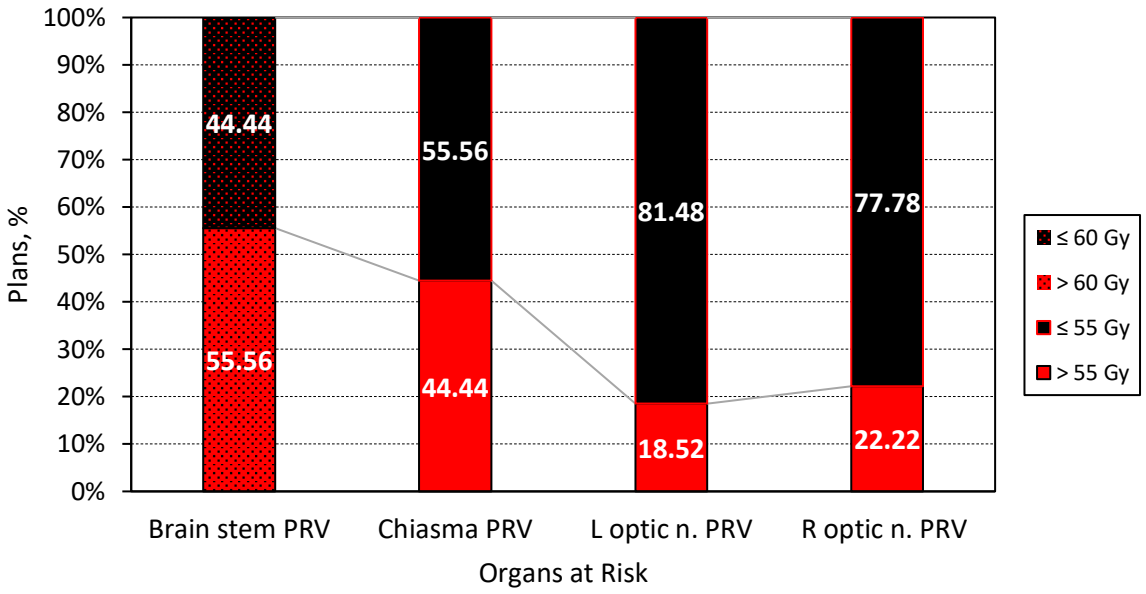

Fig. 13. Percentage of plans for which original dose constraints were exceeded (red) or reached (black) after adding PRV

According to the dose constraints provided by DAHANCA, the maximum dose to the PRVs of the selected OARs should not exceed 60 Gy. After adding a 3 mm margin around the brain stem, in 55.56 % of treatment plans maximum PRV dose constraints were exceeded (Fig. 14). For chiasma dose constraints were exceeded in 22.22 % of plans. Better results were obtained for optic nerves, where constraints were not met in 7.41 % and 11.11 % of plans for the left and right optic nerves, respectively. For chiasma and optic nerves, doses above 60 Gy are linked with more than 7 % to 20 % toxicity risks [79]

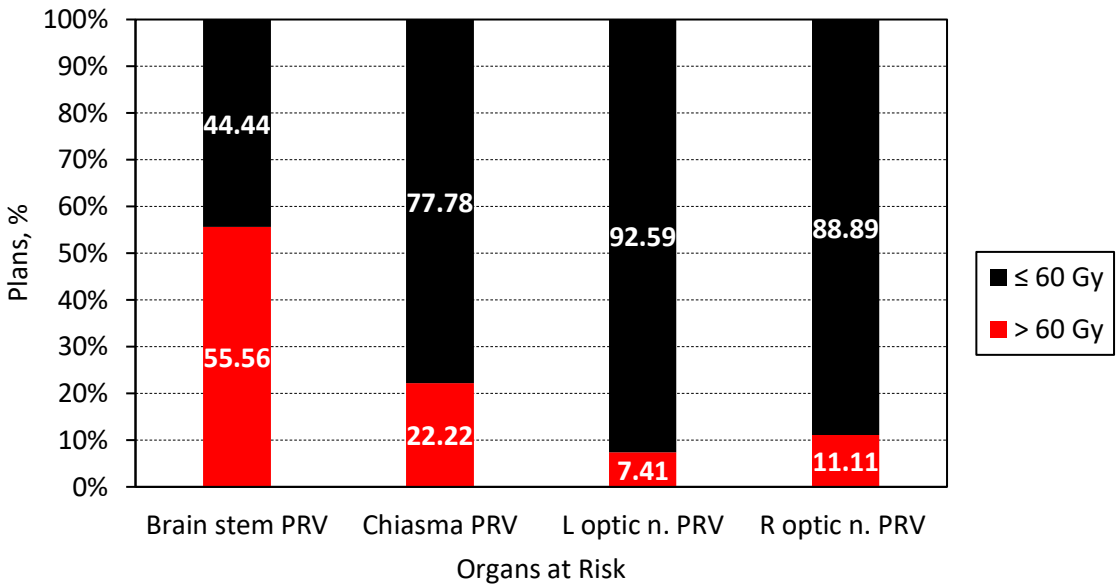

Fig. 14. Plans for which PRV dose constraints were exceeded (red) or met (black) after adding PRV

In 3 modified plans out of 27, dose constraints were exceeded for three structures, dose constraints for two structures were exceeded in 5 plans, a single structure received higher than the maximum allowed dose in 7 plans, and finally, in 12 plans all structures with PRV conformed to the set dose constraints.

Fig. 15 shows the DVH of a plan where the target was located on the left side of the temporal lobe, therefore, close to the brain stem, chiasma and the left optical nerve. PRVs of all these structures received doses greater than 60 Gy. After adding 3 mm to the structures, the maximum dose to the left optic nerve increased from 52.09 Gy up to 60.09 Gy, the dose to chiasma increased from 54.24 Gy up to 60.21 Gy and the dose received by the brain stem increased from 59.31 Gy up to 62.47 Gy.

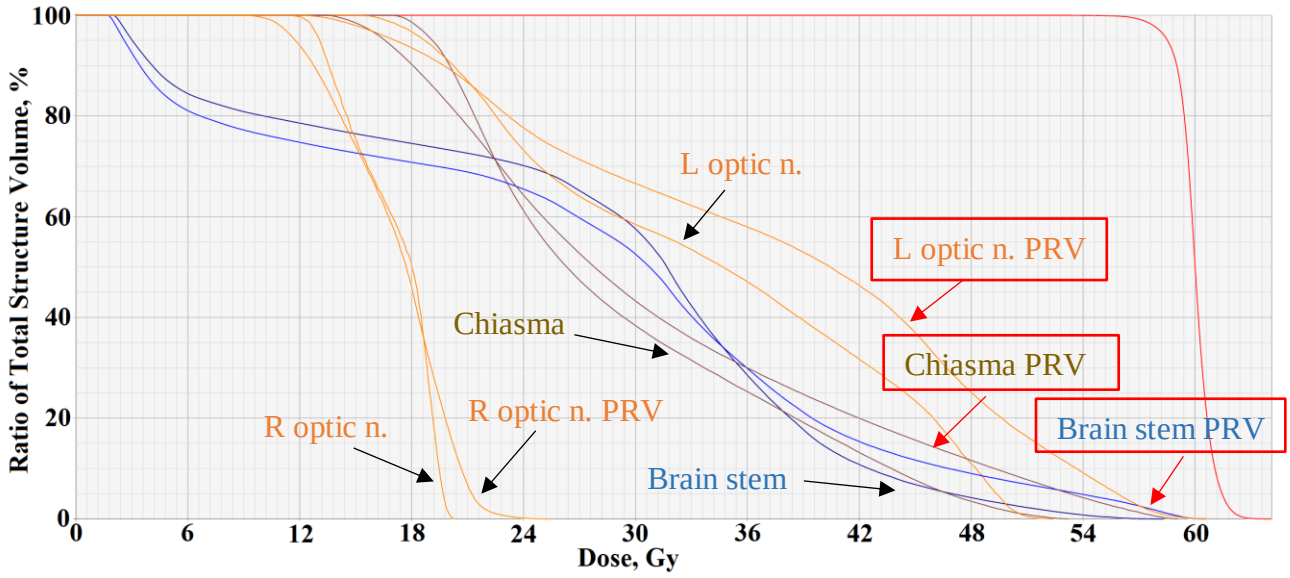

Fig. 15. DVH of a plan where PRVs of the left optic nerve, chiasma and brain stem exceeded dose constraints (DVH lines marked with red arrows)

In another plan, the target was located in the left temporal lobe. In this case, two structures, PRVs of the brainstem and the left optic nerve, exceeded dose constraints (Fig. 16). The dose to the left optic nerve increased from 52.42 Gy up to 60.75 Gy. Since the target was already close to the brain stem, the maximum dose to this structure increased only by 2.25 Gy (from 58.37 Gy up to 60.62 Gy).

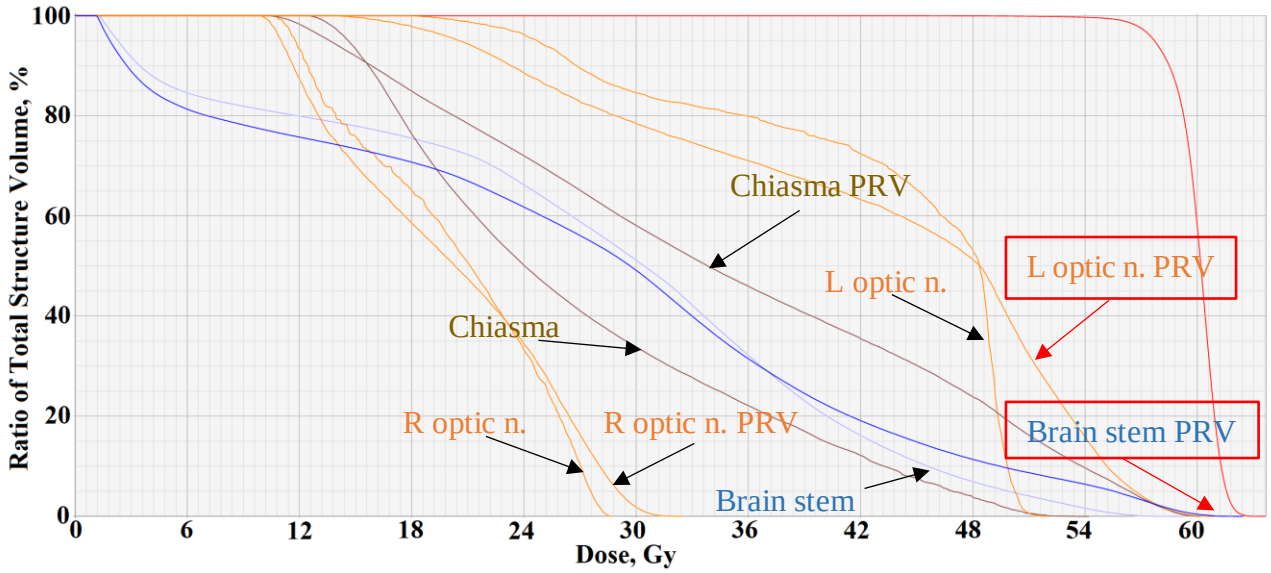

Fig. 16. DVH of a plan where PRVs of the left optic nerve and brain stem exceeded dose constraints (DVH lines marked with red arrows)

When a tumour is located in the central brain, finding the balance between the required target coverage and meeting dose constraints for the brain stem is a challenging task. Fig. 17 shows a DVH of a plan where the brain stem received 59.97 Gy, and after adding a 3 mm margin, the PRV of the brainstem received a maximum dose of 61.83 Gy. Doses delivered to PRV of the chiasma left optic

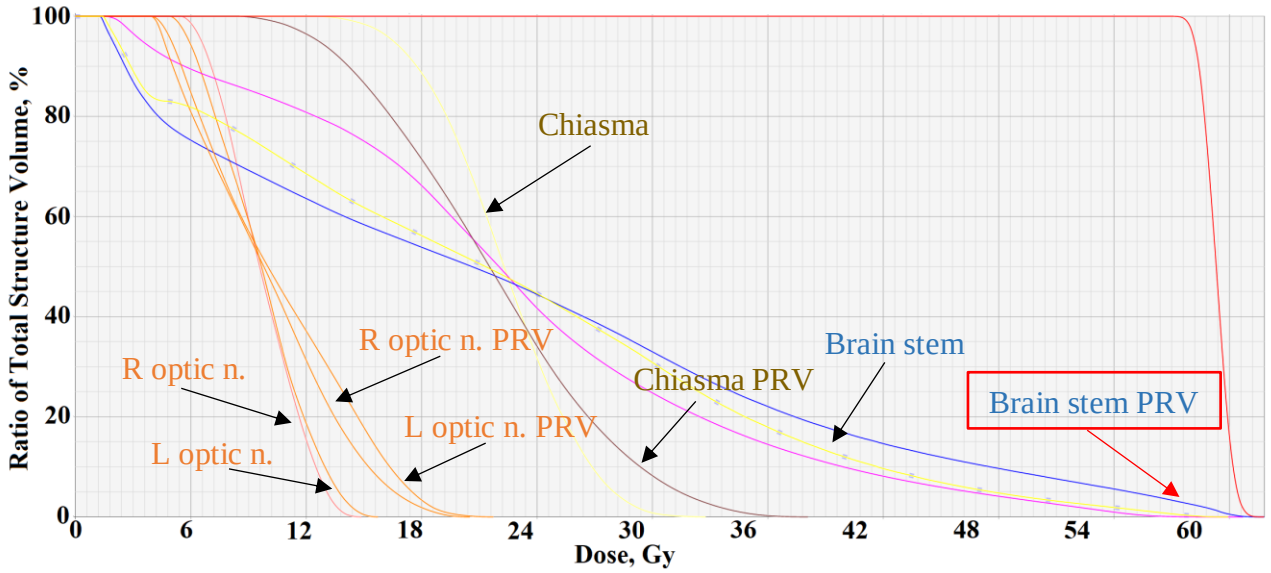

Fig. 17. DVH of a plan where PRV of the brain stem exceeded dose constraints (DVH line marked with a red arrow)

For the rest 12 plans, all dose constraints to the selected OARs were met. A DVH of one of these plans is presented below (Fig. 18). In this plan maximum dose delivered to the brain stem was 45.33 Gy, while the PRV of the brain stem received a maximum dose of 58.48 Gy. Chiasma and chiasma PRV received maximum doses of 22.16 Gy and 24.14 Gy, respectively. Maximum delivered doses to the PRVs of the optic nerves were 10.20 Gy and 10.19 Gy for the left and right optic nerves, respectively.

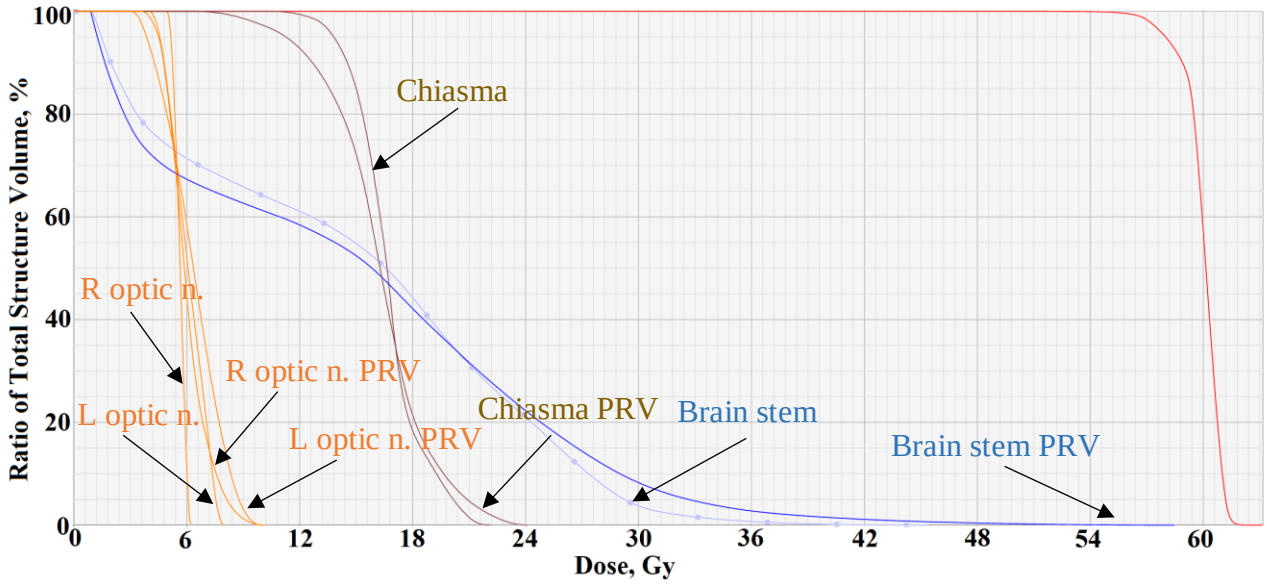

Fig. 18. DVH of a plan where PRVs of all the structures met dose constraints

3.3. Re-planning and Dose Risk Evaluation

After the re-planning, maximum doses were reduced in most of the plans. The mean maximum dose received by the brain stem was reduced from 43.79 Gy in the original plans down to 40.71 Gy in the re-planned plans (Fig. 19). Dose reduction was achieved in 21 plans out of 27. In 3 plans (Fig. 19, patients 14, 15, and 18) doses delivered to the brain stem were slightly higher than in original plans. The increase mostly resulted due to the competition between sparring different normal tissues while still trying to reach at least 95 % PTV coverage. For the other 3 plans (Fig. 19, patients 24, 25 and 27) increase was negligible and received doses were well below dose constraints.

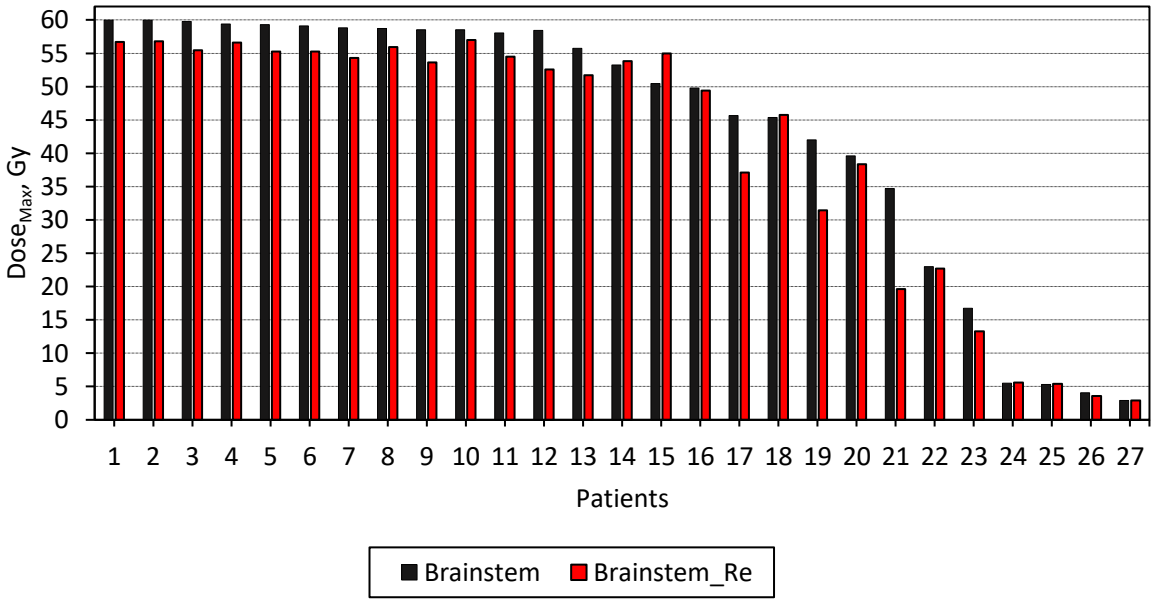

Fig. 19. Maximum doses delivered to the brain stem in the original (black) and re-planned (red) plans

According to the protocol implemented in the clinic, the brain stem is separated into two structures, surface and interior. The interior part is obtained by applying a 2 mm inner margin to the brain stem; the surface is obtained by subtracting the interior part from the whole brain stem volume. The maximum dose constraint for the brain stem interior and surface are 54 Gy and 60 Gy, respectively.

PRV margin was added to the whole brain stem structure, thus the interior part was optimized following the usual protocol. Despite that, in 18 re-planned plans maximum doses delivered to the brain stem interior also were lower in comparison to the original plans (Fig. 20). Mean maximum dose in the original plans was 34.97 Gy, while in the re-planned plans mean maximum dose was reduced down to 33.34 Gy.

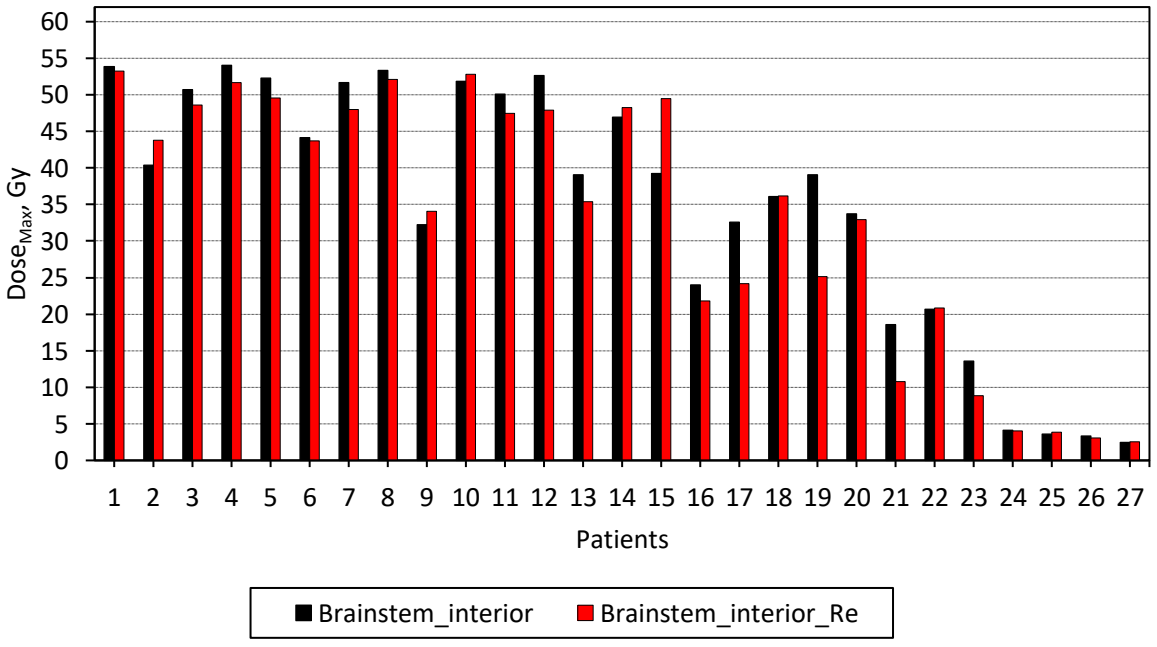

Fig. 20. Maximum doses delivered to the brain stem interior in the original (black) and re-planned (red) plans

For chiasma, re-optimization led to a reduced maximum dose in 22 plans (Fig. 21). Mean maximum dose after re-optimization was lowered from 30.91 Gy down to 28.27 Gy. The maximum dose of chiasma slightly increased for 5 patients. For patient 2, the dose to chiasma increased by 1.50 Gy, however maximum doses to the brain stem and both optic nerves were reduced.

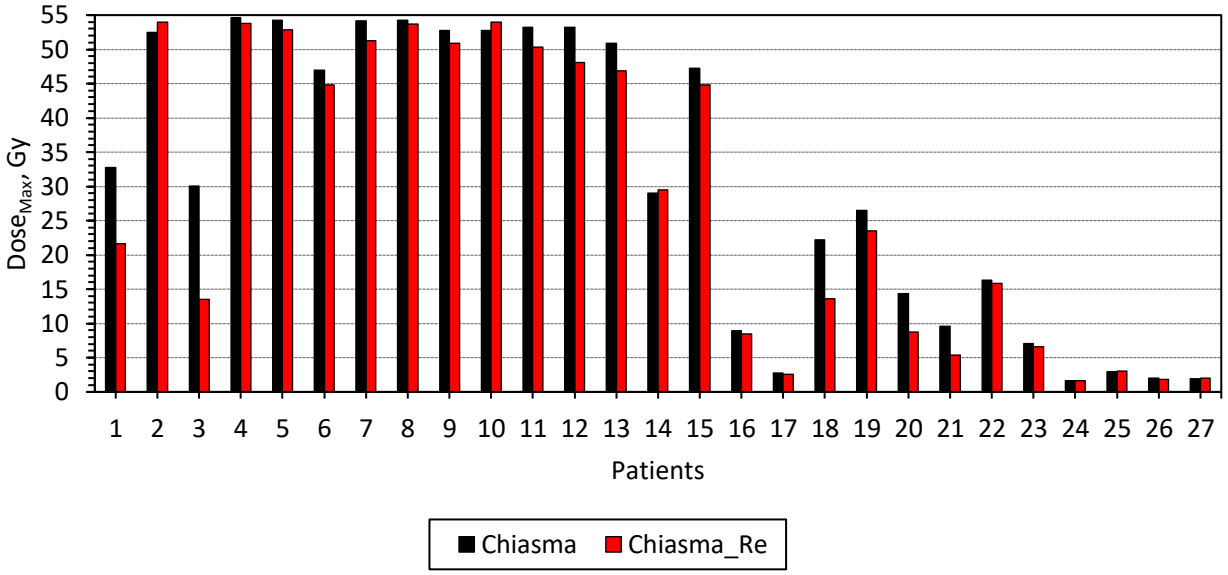

Fig. 21. Maximum doses delivered to the chiasma in the original (black) and re-planned (red) plans

For the left optic nerve, dose reduction was achieved in 23 re-planned treatment plans (Fig. 22). The highest increase of 1.69 Gy was observed for patient no. 12, however as the maximum dose was 21.00 Gy, it's still below the tolerance dose of 55 Gy. Overall, the mean maximum dose was reduced by 2.27 Gy from 21.83 Gy down to 19.56 Gy.

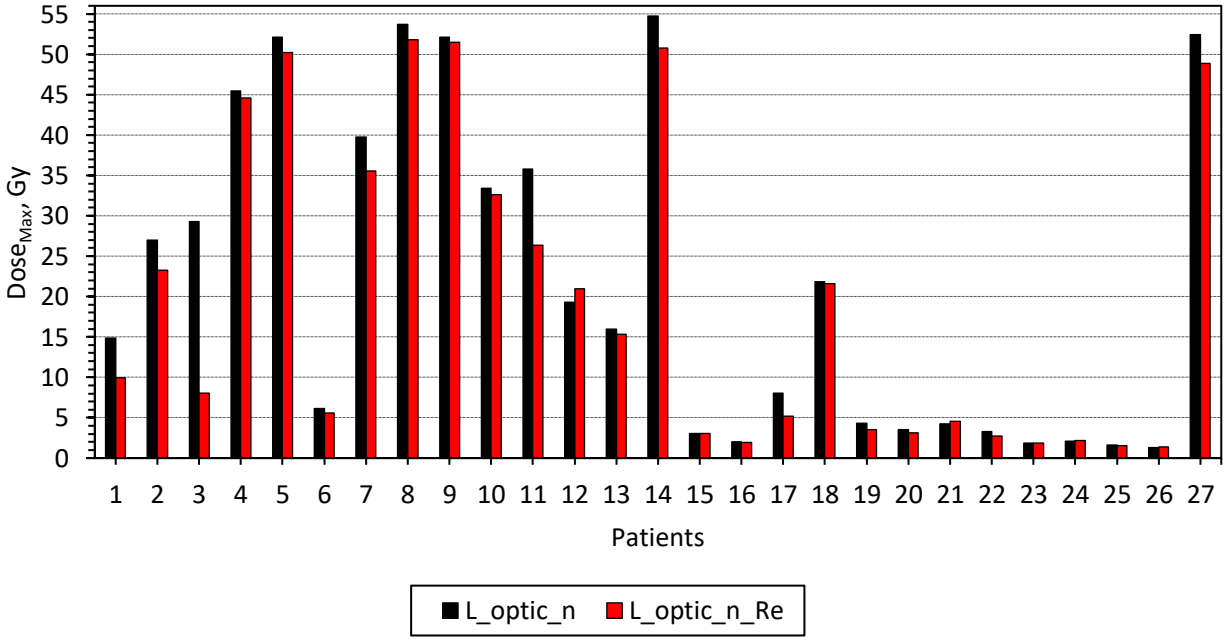

Fig. 22. Maximum doses delivered to the left optic nerve in the original (black) and re-planned (red) plans

The mean maximum dose to the right optic nerve was reduced by 1.69 Gy, from 19.54 Gy down to 17.85 Gy. In total dose reduction was achieved in 19 plans (Fig. 23). For patient 18, after re-planning, the dose to the right optic nerve increased by 2.35 Gy, however doses to the brain stem, chiasma and left optic nerve were reduced by 10.58 Gy, 2.96 and 0.17 Gy, respectively.

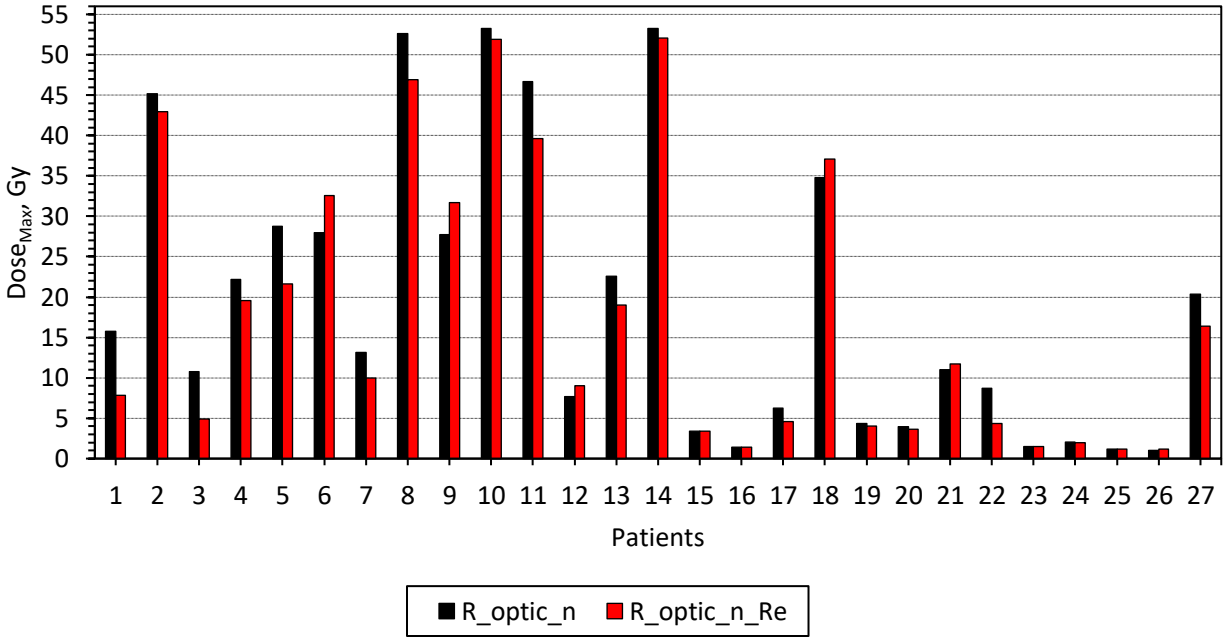

Fig. 23. Maximum doses delivered to the right optic nerve in the original (black) and re-planned (red) plans

Besides lowering doses to the selected OARs, another objective was to maintain appropriate PTV coverage. According to the implemented protocol, 95 % of the target volume had to receive at least 95 % of the total prescribed dose. This objective was successfully achieved in all re-planned plans (Fig. 24). For thirteen plans, PTV coverage after the re-planning was even higher than in original plans by 0.06 %– 3.68 %.

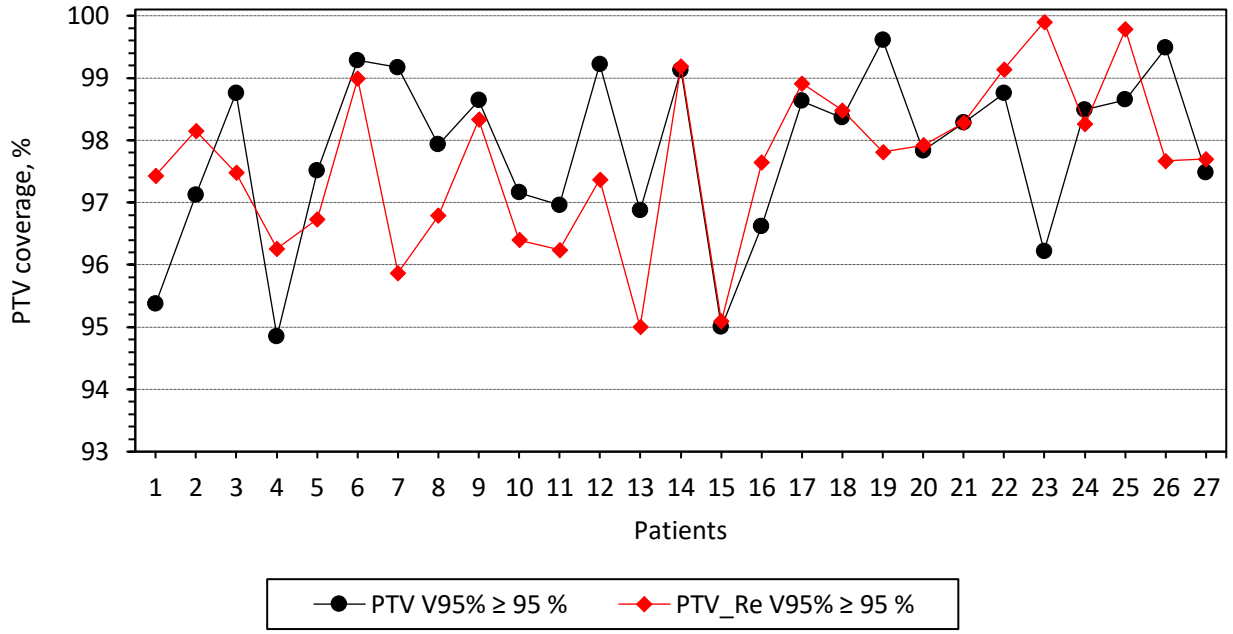

Fig. 24. PTV coverage in the original (black) and the re-planned (red) plans

The mean minimum dose for the re-planned plans was 46.32 Gy, while for original plans – 48.59 Gy. The mean minimum dose for the re-planned plans was 46.32 Gy, while for original plans – 48.59 Gy. It was observed that after re-planning minimum PTV dose increased by 0.49 – 5.17 Gy in 9 plans and decreased in 17 plans (Fig. 25). For the majority of the plans, the decrease was between 0.11 Gy and 5.52 Gy, however for plans 11 and 13 minimum doses decreased by 26.23 Gy and 11.32 Gy, respectively. For plans, where the target is closely surrounded by OARs from different directions, adding PRV margins complicates the optimization and results in worse PTV coverage as shown in Fig. 26. PTV coverage in such situations could be improved by applying more sophisticated optimization algorithms and by optimal priority values for PTV and organs at risk.

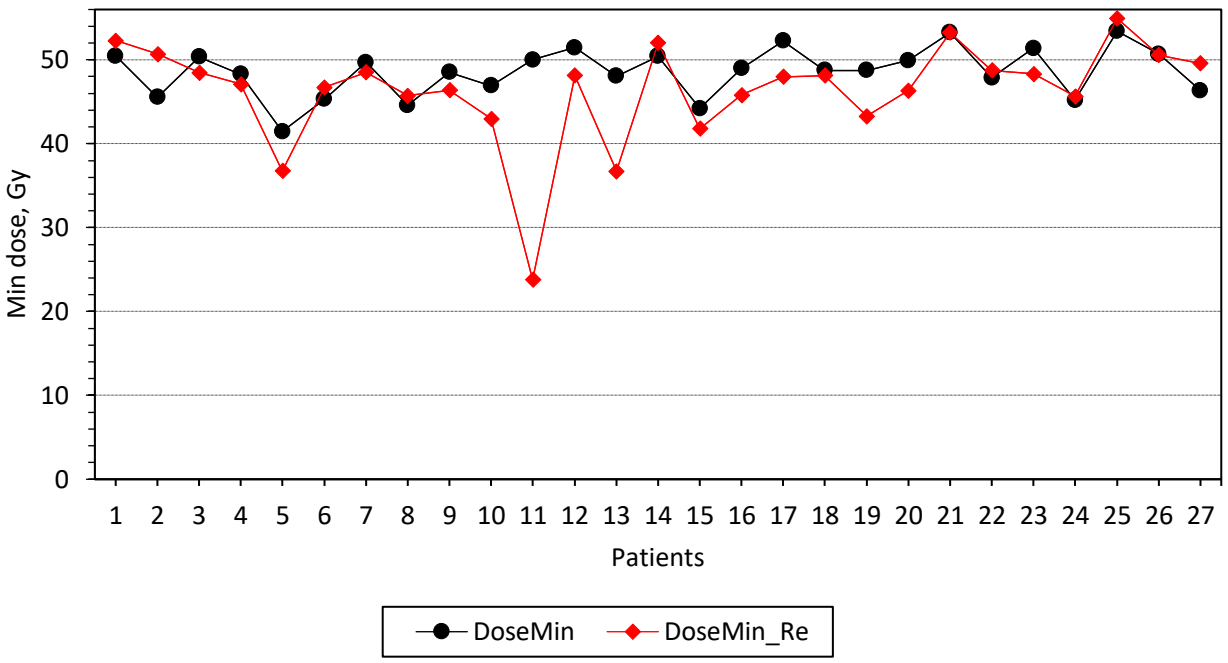

Fig. 25. Minimum dose delivered to the PTV in the original (black) and the re-planned (red) plans

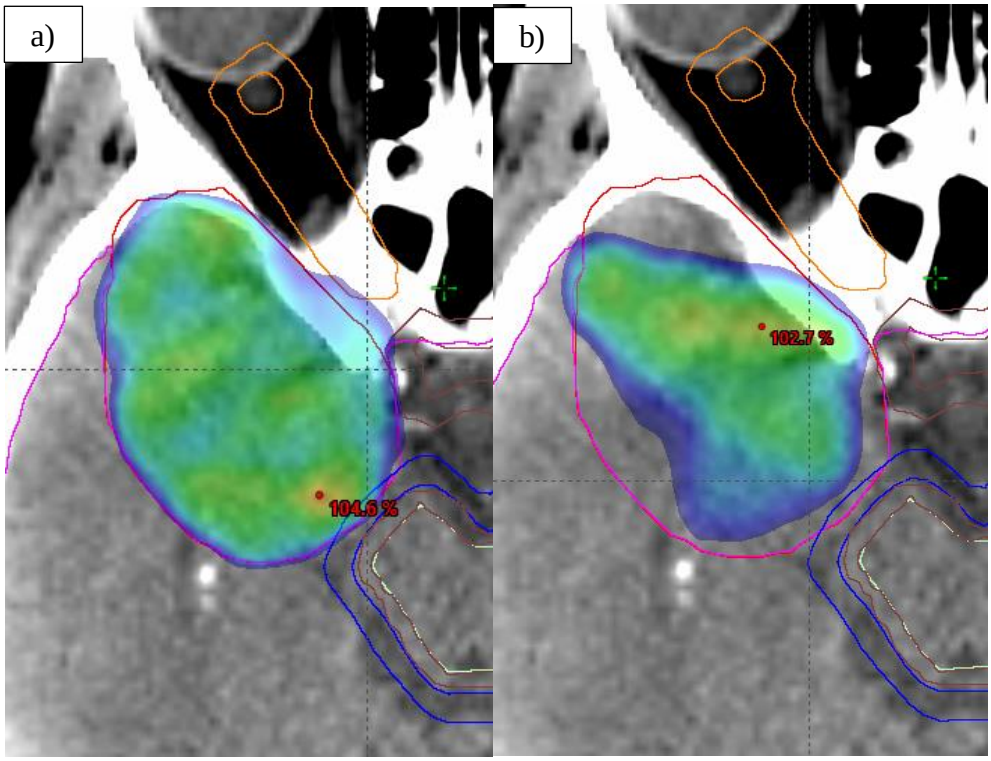

Fig. 26. PTV coverage with a 95% isodose line (a) in the original plan and (b) after re-planning

The quality of the re-planned plans also was assessed using a conformity index (CI). A conformity index of 1.00 indicates ideal PTV coverage. A CI of less than 1.00 shows that the target is covered only partially, while a CI of more than 1.00 means that the prescribed dose exceeds the boundaries of the target volume. The mean CI of the re-planned plans was 0.60, while the CI of the original plans was slightly lower, 0.57 (Fig. 27). Therefore, implementation of PRV did not cause any significant deterioration in plan conformity.

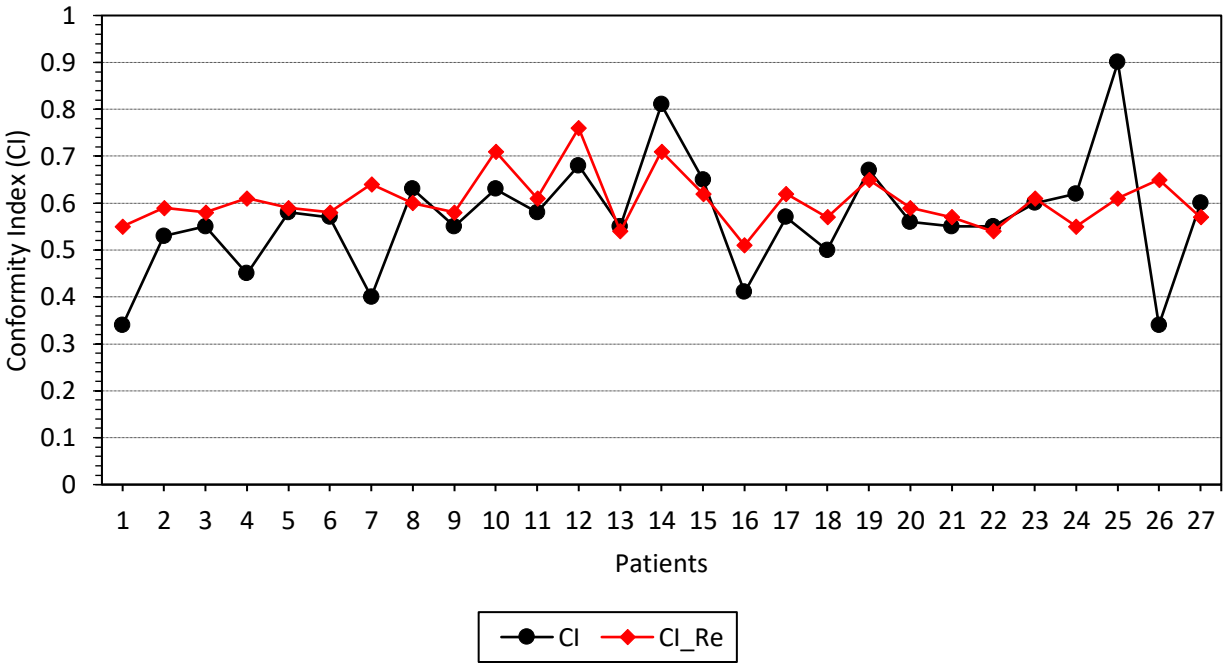

Fig. 27. PTV conformity index in the original (black) and the re-planned (red) plans

3.4. Evaluation of Uncertainty Plans

15 re-planned high-risk plans that did not pass PRV constraints in the original plans were additionally evaluated by shifting the isocenter by ± 3 mm to the reference position. For each plan, 6 uncertainty plans were generated. 6 out of 15 of the re-planned plans passed all the dose constraints to the selected OARs. Uncertainty plans of the rest 9 re-planned plans met dose constraints only partially.

The mean maximum dose for each structure with different positional shifts is presented in Fig. 28. Brainstem received a mean maximum dose of 57.66 Gy when the isocenter was shifted by –3 mm in the z-direction. The mean maximum dose for chiasma varied between 42.48 Gy (+3 mm in y) and 48.23 Gy (-3 mm in z). For the left optic nerve, noticeably higher mean maximum doses of 32.61 Gy, 34.53 Gy and 37.29 Gy were delivered when the isocenter was shifted by –3 mm in x, y and z directions, respectively. For the right optic nerve, higher doses of 31.66 Gy and 30.90 Gy were observed when the isocenter was shifted by ± 3 mm in the z-direction. Shifting the isocenter by +3 mm in the y-direction increased the dose to the brain stem and reduced the dose to all the other structures.

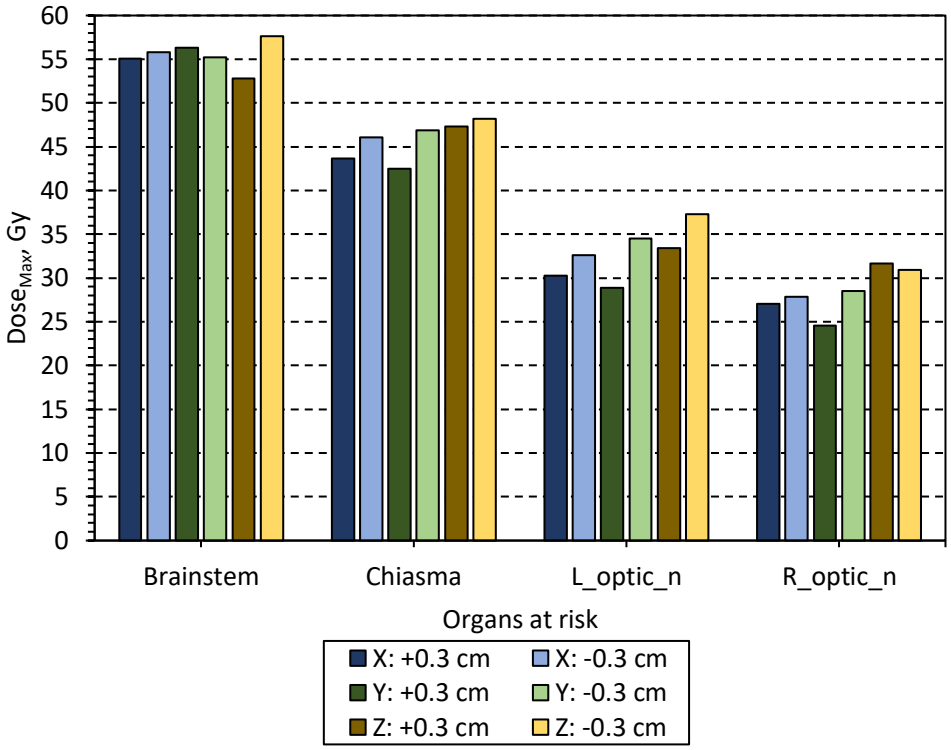

Fig. 28. Mean maximum doses received by the brain stem, chiasma, and optic nerves in uncertainty plans in different directions

Fig. 29 shows uncertainty plans that exceeded tolerance doses for the brain stem, chiasma and optic nerves depending on the direction to which the isocenter was shifted. Brain stem did not exceed 60 Gy tolerance dose in any of the uncertainty plans. Left and right optic nerves received higher than allowed doses in 8 and 4 out of 90 uncertainty plans, respectively. Tolerance doses for chiasma were exceeded in 24 plans. Such a high number of plans in comparison with other structures can be due to chiasma location and tolerance dose. Since chiasma is located at the base of the brain, there is a higher chance for a tumour to be closer to the chiasma than optic nerves. According to the protocol applied in the clinic, the maximum allowed dose for chiasma is 55 Gy, while for the brain stem surface, it is 60 Gy. With the total prescribed dose being 60 Gy, there is a higher risk for the 55 Gy constraint to be exceeded.

Analysis of uncertainty plans revealed that isocenter shifts along the z-direction result in the highest maximum doses and highest number of structures receiving greater than allowed doses (Fig. 29). This tendency is also associated with tumour location with respect to organs at risk. Target is significantly larger than the organs at risk, therefore, by shifting the isocenter along the z-direction (vertically), the dose intended for the tumour crosses the plane where the organs at risk are situated (Fig. 30).

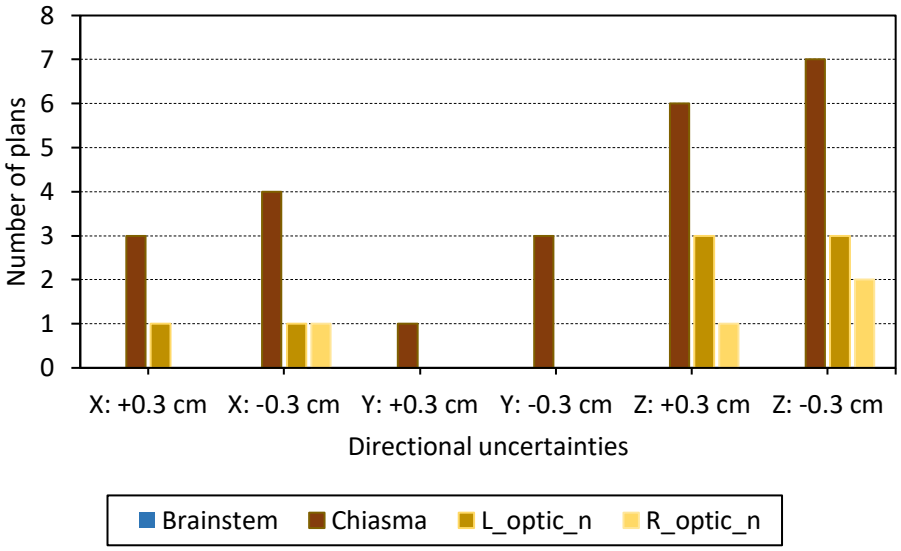

Fig. 29. Number of uncertainty plans that did not pass dose constraints for the brain stem, chiasma, and optic nerves in respect to positional isocenter shifts

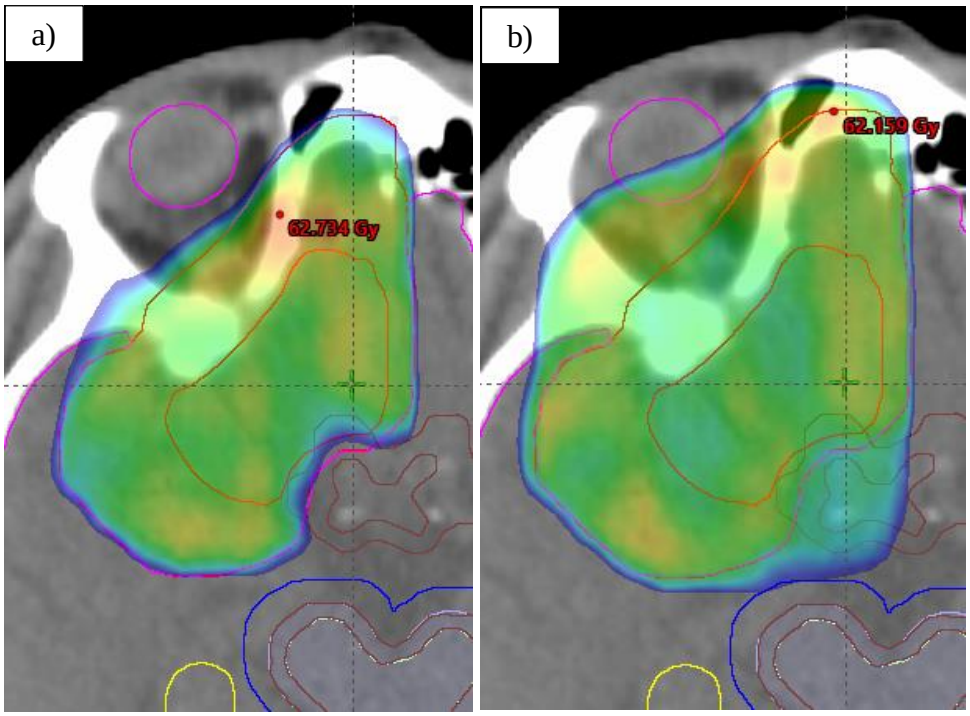

Fig. 30. PTV coverage with a 55 Gy isodose line (a) in the re-planned plan and (b) after a -3 mm shift in the z-direction

Conclusions

1. Greatest mean set-up uncertainties of -1.88 mm (TRUEBEAM) and 2.06 mm (TRILOGY) were observed in the vertical direction. For TRUEBEAM systematic uncertainties varied between 1.43 – 1.56 mm and between 0.75 – 1.63 mm for TRILOGY. Using McKenzie's et al. formula, calculated PRV margins for TRUEBEAM were between 2.51 – 2.58 mm, and between 1.47 mm and 2.70 mm for TRILOGY. Using Stroom's et al. formula, PRV margins were slightly larger, 2.54 – 2.72 mm, 1.39 – 2.84 mm for TRUEBEAM and TRILOGY, respectively.
2. Initially, planning organ at risk volumes of the selected organs at risk (brain stem, chiasma and optic nerves) received significantly higher maximum doses than the structures. PRV tolerance doses were exceeded in 55.56 %, 22.22 %, 7.41 % and 11.11 % plans for the PRVs of the brain stem, chiasma, left optic nerve and right optic nerve, respectively. After re-planning all plans met PRV tolerance doses and mean maximum doses to the brain stem, chiasma, right optic nerve and left optic nerve were reduced by 3.08 Gy, 2.64 Gy, 2.27 Gy and 1.69 Gy, respectively.
3. In most of the re-planned plans, planning dose risk was reduced without compromising PTV coverage. On average, in the original plans, 95 % of the prescribed dose was delivered to 97.83 % of the target volume. After re-planning, the mean PTV volume covered by 95 % of the prescribed dose decreased only negligibly by 0.17 % down to 97.66 %. The conformity index also did not show any decrease in the plan quality as the mean conformity index of original and re-planned plans was 0.57 and 0.60, respectively. The mean minimum PTV dose for original plans and re-planned plans was 48.59 Gy and 46.32 Gy. The decrease in the mean minimum dose was influenced by 3 out of 27 re-planned plans, for which, due to the close vicinity to several organs at risk, the minimum dose to the PTV was below 40 Gy.
4. Generation of ± 3 mm uncertainty plans led to an increase in the mean maximum dose by 1.30 Gy, 1.02 Gy 1.08 Gy and 1.13 Gy for the brain stem, chiasma, left optic nerve and the right optic nerve, respectively. The brain stem did not exceed the tolerance dose in any of the uncertainty plans. Tolerance doses for chiasma were exceeded in 24 out of 90 plans. For the left and right optic nerves, tolerance doses were exceeded only in 8 and 4 uncertainty plans, respectively. Most tolerance doses were exceeded when the patient's set-up was shifted by ± 3 mm along the vertical (z) direction.

List of References

1. FAN, Y., et al. Burden and trends of brain and central nervous system cancer from 1990 to 2019 at the global, regional, and country levels. *Arch Public Health* [online]. 2022, **80**(209) [viewed 3 April 2023]. Available from: doi: 10.1186/s13690-022-00965-5.
2. SUNG, H., et al. Global cancer statistics 2020: GLOBOCAN estimates of incidence and mortality worldwide for 36 cancers in 185 countries. *CA: a cancer journal for clinicians* [online]. 2021, **71**(3), 209–249 [viewed 3 April 2023]. Available from: doi: 10.3322/caac.21660.
3. HUANG, J., et al. The comparative burden of brain and central nervous system cancers from 1990 to 2019 between China and the United States and predicting the future burden. *Frontiers in public health* [online]. 2022, **10**, [viewed 3 April 2023]. Available from: doi: 10.3389/fpubh.2022.1018836.
4. OSTROM, Q. T., et al. CBTRUS Statistical Report: Primary Brain and Other Central Nervous System Tumors Diagnosed in the United States in 2011-2015. *Neuro-oncology* [online]. 2018, **20**(suppl_4), iv1–iv86 [viewed 3 April 2023]. Available from: doi:10.1093/neuonc/noy131.
5. SCARINGI, C., L. AGOLLI and G. MINNITI. Technical Advances in Radiation Therapy for Brain Tumors. *Anticancer research* [online]. 2018, **38**(11), 6041–6045 [viewed 3 April 2023]. Available from: doi: 10.21873/anticanres.12954.
6. VAN DER MERWE, D., et al. Accuracy requirements and uncertainties in radiotherapy: a report of the International Atomic Energy Agency. *Acta oncologica* [online]. 2017, **56**(1), 1–6 [viewed 3 April 2023]. Available from: doi: 10.1080/0284186X.2016.1246801.
7. AZZAM, P., et al. Radiation-induced neuropathies in head and neck cancer: prevention and treatment modalities. *Ecancermedicalscience* [online]. 2020, **14**, 1133 [viewed 3 April 2023]. Available from: doi: 10.3332/ecancer.2020.1133.
8. International Commission on Radiation Units and Measurements ICRU report 62: Prescribing, recording, and reporting photon beam therapy (supplement to ICRU report 50). *International Commission on Radiation Units and Measurements*, Bethesda, 1999.
9. International Commission on Radiation Units and Measurements. ICRU Report 83, Prescribing, Recording, and Reporting Intensity-Modulated Photon-Beam Therapy (IMRT). *Journal of the ICRU* [online]. 2010, **14**(1), [viewed 3 April 2023]. Available from: doi: 10.1093/jicru/ndw040.
10. International Commission on Radiation Units and Measurements ICRU report 50: Prescribing, recording, and reporting photon beam therapy. *International Commission on Radiation Units and Measurements*, Washington (DC), 1993.
11. HALL, E. J., and C. S. WUU. Radiation-induced second cancers: the impact of 3D-CRT and IMRT. *International journal of radiation oncology, biology, physics* [online]. 2003, **56**(1), 83–88 [viewed 20 March 2023]. Available from: doi: 10.1016/s0360-3016(03)00073-7.
12. CHEN, M.J., et al. Intensity-Modulated and 3D-Conformal Radiotherapy for Whole-Ventricular Irradiation as Compared with Conventional Whole-Brain Irradiation in the Management of Localized Central Nervous System Germ Cell Tumors. *International journal of radiation oncology, biology, physics* [online]. 2010, **76** (2), 608-614 [viewed 20 March 2023]. Available from: doi: 10.1016/j.ijrobp.2009.06.028.
13. NAGARAJAN, M., et al. Dosimetric Evaluation and Comparison Between Volumetric Modulated Arc Therapy (VMAT) and Intensity Modulated Radiation Therapy (IMRT) Plan in

Head and Neck Cancers. *The Gulf Journal of Oncology* [online]. 2020, **1**(33), 45–50 [viewed 20 March 2023]. Available from: PMID: 32476649.

14. HOLT, A., et al. Multi-institutional comparison of volumetric modulated arc therapy vs. intensity-modulated radiation therapy for head-and-neck cancer: a planning study. *Radiation oncology* [online]. 2013, **8**(26) [viewed 20 March 2023]. Available from: doi: 10.1186/1748-717X-8-26.
15. BALLHAUSEN, H., et al. Shorter treatment times reduce the impact of intra-fractional motion: A real-time 4DUS study comparing VMAT vs. step-and-shoot IMRT for prostate cancer. *Strahlentherapie und Onkologie* [online]. 2018, **194**(7), 664–674 [viewed 20 March 2023]. Available from: doi: 10.1007/s00066-018-1286-2.
16. BEYZADEOGLU, M., et al. Radiobiology. In: BEYZADEOGLU, M. et al. *Basic Radiation Oncology* [online]. Cham (ZG): Springer, 2022, pp. 47–97 [viewed 20 May 2023]. ISBN 978-3-030-87308-0. Available from: doi: https://doi.org/10.1007/978-3-030-87308-0_2.
17. SULTANA, N., et al. Biomarkers of Brain Damage Induced by Radiotherapy. *Dose-response: a publication of International Hormesis Society* [online]. 2020, **18**(3) [viewed 20 May 2023]. Available from: doi: 10.1177/1559325820938279.
18. JACOB, J., et al. Cognitive impairment and morphological changes after radiation therapy in brain tumors: A review. *Radiotherapy and Oncology* [online]. 2018, **128**(2), 221–228 [viewed 20 May 2023]. Available from: doi: 10.1016/j.radonc.2018.05.027.
19. MEYERS, C.A., et al. Neurocognitive function and progression in patients with brain metastases treated with whole-brain radiation and motexafin gadolinium: results of a randomized phase III trial. *Journal of clinical oncology: official journal of the American Society of Clinical Oncology* [online]. 2004, **22**(1), 157-165 [viewed 20 May 2023]. Available from: doi: 10.1200/JCO.2004.05.128.
20. BRANDSMA, D., et al. Clinical features, mechanisms, and management of pseudoprogression in malignant gliomas. *The Lancet. Oncology* [online]. 2008, **9**(5), 453–461 [viewed 20 May 2023]. Available from: doi: 10.1016/S1470-2045(08)70125-6.
21. KUMAR, A. J., et al. Malignant gliomas: MR imaging spectrum of radiation therapy – and chemotherapy-induced necrosis of the brain after treatment. *Radiology* [online]. 2000, **217**(2), 377–384 [viewed 20 May 2023]. Available from: doi: 10.1148/radiology.217.2.r00nv36377.
22. RUBEN, J. D., et al. Cerebral radiation necrosis: incidence, outcomes, and risk factors with emphasis on radiation parameters and chemotherapy. *International journal of radiation oncology, biology, physics* [online]. 2006, **65**(2), 499–508 [viewed 20 May 2023]. Available from: doi: 10.1016/j.ijrobp.2005.12.002.
23. KATSURA. M., et al. Recognizing Radiation-induced Changes in the Central Nervous System: Where to Look and What to Look for. *Radiographics* [online]. 2021, **41**(1), 224-248 [viewed 20 May 2023]. Available from: doi: 10.1148/rg.2021200064.
24. LAMBRECHT, M., et al. Work package 1 of the task force "European Particle Therapy Network" of ESTRO. Radiation dose constraints for organs at risk in neuro-oncology; the European Particle Therapy Network consensus. *Radiotherapy and oncology: journal of the European Society for Therapeutic Radiology and Oncology* [online]. 2018, **128**(1), 26–36 [viewed 7 April 2023]. Available from: doi: 10.1016/j.radonc.2018.05.001.
25. PDQ Adult Treatment Editorial Board. Adult Central Nervous System Tumors Treatment (PDQ®): Health Professional Version. In: *PDQ Cancer Information Summaries* [online].

Bethesda (MD): National Cancer Institute (US); 2002 [viewed 7 April 2023]. Available from: https://www.ncbi.nlm.nih.gov/books/NBK65982/

26. LAWRENCE, Y. R., et al. Radiation dose-volume effects in the brain. *International journal of radiation oncology, biology, physics* [online]. 2010, **76**(3 Suppl), S20–S27 [viewed 7 April 2023]. Available from: doi: 10.1016/j.ijrobp.2009.02.091.
27. KIM, S. E., et al. Effects of radiation therapy on the meibomian glands and dry eye in patients with ocular adnexal mucosa-associated lymphoid tissue lymphoma. *BMC ophthalmology* [online]. 2020, **20**(24) [viewed 7 April 2023]. Available from: doi: 10.1186/s12886-019-1301-0.
28. GORE, S. K., et al. Corneal complications after orbital radiotherapy for primary epithelial malignancies of the lacrimal gland. *The British Journal of Ophthalmology* [online]. 2018, **102**(7), 882–884 [viewed 7 April 2023]. Available from: doi: 10.1136/bjophthalmol-2017-311134.
29. FERRUFINO-PONCE, Z. K., and B. A. HENDERSON. Radiotherapy and cataract formation. *Seminars in ophthalmology* [online]. 2006, **21**(3), 171–180 [viewed 7 April 2023]. Available from: doi: 10.1080/08820530500351728.
30. WANG, W. Radiation-induced optic neuropathy following external beam radiation therapy for nasopharyngeal carcinoma: A retrospective case-control study. *Molecular and clinical oncology*, [online]. 2016, **4**(5), 868–872 [viewed 7 April 2023]. Available from: doi: 10.3892/mco.2016.787
31. BHANDARE, N., et al. Does altered fractionation influence the risk of radiation-induced optic neuropathy? *International journal of radiation oncology, biology, physics* [online]. 2005, **62**(4), 1070–1077 [viewed 7 April 2023]. Available from: doi: 10.1016/j.ijrobp.2004.12.009.
32. PAN, C. C., et al. Prospective study of inner ear radiation dose and hearing loss in head-and-neck cancer patients. *International journal of radiation oncology, biology, physics* [online]. 2005, **61**(5), 1393–1402 [viewed 7 April 2023]. Available from: doi: 10.1016/j.ijrobp.2004.08.019.
33. DOUW, L., et al. Cognitive and radiological effects of radiotherapy in patients with low-grade glioma: long-term follow-up. *The Lancet. Neurology* [online]. 2009, *8*(9), 810–818 [viewed 7 April 2023]. Available from: doi: 10.1016/S1474-4422(09)70204-2.
34. AGHA, A., et al. Hypothalamic-pituitary dysfunction after irradiation of nonpituitary brain tumours in adults. *The Journal of clinical endocrinology and metabolism* [online]. 2005, **90**(12), 6355–6360 [viewed 7 April 2023]. Available from: doi: 10.1210/jc.2005-1525.
35. BHANDARE, N., et al. Radiation therapy and hearing loss. *International journal of radiation oncology, biology, physics* [online]. 2020, **76**(3 Suppl), S50–S57 [viewed 10 April 2023]. Available from: doi: 10.1016/j.ijrobp.2009.04.096.
36. THARIAT, J., et al. Non-Cancer Effects Following Ionizing Irradiation Involving the Eye and Orbit. *Cancers* [online]. 2022, **14**(5), 1194 [viewed 10 April 2023]. Available from: doi: 10.3390/cancers14051194.
37. NIYAZI, M., et al. ESTRO-ACROP guideline "target delineation of glioblastomas". *Radiotherapy and oncology: journal of the European Society for Therapeutic Radiology and Oncology* [online]. 2016, **118**(1), 35–42 [viewed 10 April 2023]. Available from: doi: 10.1016/j.radonc.2015.12.003.
38. JENSEN, K., et al. The Danish Head and Neck Cancer Group (DAHANCA) 2020 radiotherapy guidelines. *Radiotherapy and oncology: journal of the European Society for Therapeutic Radiology and Oncology* [online]. 2020, **151**(October), 149–151 [viewed 10 April 2023]. Available from: doi: 10.1016/j.radonc.2020.07.037. DAHANCA_Radiotherapy_guidelines_2020.

39. BENEDICT, S. H., et al. Stereotactic body radiation therapy: the report of AAPM Task Group 101. *Medical physics* [online]. 2010, **37**(8), 4078–4101 [viewed 10 April 2023]. Available from: doi: 10.1118/1.3438081.
40. MAKKINJE, A. *Characterizing the effects of delineation uncertainties in head and neck cancer radiotherapy* [online]. Master thesis, Delft University of Technology, 2023 [viewed 10 April 2023]. Available from: http://resolver.tudelft.nl/uuid:81930e0e-f0aa-41dc-a07a-27c6761025a8.
41. SHUSHARINA, N., et al. Accounting for uncertainties in the position of anatomical barriers used to define the clinical target volume. *Physics in medicine and biology* [online]. 2021, **66**(15) [viewed 14 April 2023]. Available from: doi: 10.1088/1361-6560/ac0ea3.
42. VAN KRANEN, S., et al. Setup uncertainties of anatomical sub-regions in head-and-neck cancer patients after offline CBCT guidance. *International journal of radiation oncology, biology, physics* [online]. 2009, **73**(5), 1566–1573 [viewed 14 April 2023]. Available from: doi: 10.1016/j.ijrobp.2008.11.035.
43. Segedin, B. and P. Petric. Uncertainties in target volume delineation in radiotherapy – are they relevant and what can we do about them? *Radiology and Oncology* [online]. 2016, **50**(3) 254-262 [viewed 14 April 2023]. Available from: doi: 10.1515/raon-2016-0023.
44. STROOM, J. C., and B. J. HEIJMEN. Limitations of the planning organ at risk volume (PRV) concept. *International journal of radiation oncology, biology, physics* [online]. 2006, **66**(1), 279–286 [viewed 14 April 2023]. Available from: doi: 10.1016/j.ijrobp.2006.05.009.
45. STROOM, J. C., and B. J. HEIJMEN. Geometrical uncertainties, radiotherapy planning margins, and the ICRU-62 report. *Radiotherapy and oncology: journal of the European Society for Therapeutic Radiology and Oncology* [online]. 2002, **64**(1), 75–83 [viewed 14 April 2023]. Available from: doi: 10.1016/s0167-8140(02)00140-8.
46. KAPLAN, L. P., et al. Plan quality assessment in clinical practice: Results of the 2020 ESTRO survey on plan complexity and robustness. *Radiotherapy and oncology: journal of the European Society for Therapeutic Radiology and Oncology* [online]. 2022, **173**(August), 254–261 [viewed 17 March 2023]. Available from: doi: 10.1016/j.radonc.2022.06.005.
47. DELISHAJ, D., et al. Set-up errors in head and neck cancer treated with IMRT technique assessed by cone-beam computed tomography: a feasible protocol. *Radiation oncology journal* [online]. 2018, **36**(1), 54–62 [viewed 17 March 2023]. Available from: doi: 10.3857/roj.2017.00493.
48. PURDY, J. A. Current ICRU definitions of volumes: limitations and future directions. *Seminars in radiation oncology* [online]. 2014, **14**(1), 27–40 [viewed 17 March 2023]. Available from: doi: 10.1053/j.semradonc.2003.12.002.
49. FARACE, P., et al. Preventive sparing of spinal cord and brain stem in the initial irradiation of locally advanced head and neck cancers. *Journal of applied clinical medical physics* [online]. 2014, **15**(1), 4399 [viewed 17 March 2023]. Available from: doi: 10.1120/jacmp.v15i1.4399.
50. TSIEN, C. I., et al. NRG Oncology/RTOG1205: A Randomized Phase II Trial of Concurrent Bevacizumab and Reirradiation Versus Bevacizumab Alone as Treatment for Recurrent Glioblastoma. *Journal of clinical oncology: official journal of the American Society of Clinical Oncology* [online]. 2016, **41**(6), 1285–1295 [viewed 17 March 2023]. Available from: doi: 10.1200/JCO.22.00164.
51. YUAN, J., et al. Dosimetric comparison between intensity-modulated radiotherapy and RapidArc with single arc and dual arc for malignant glioma involving the parietal lobe. *Molecular and*

clinical oncology [online]. 2016, **5**(1), 181–188 [viewed 17 March 2023]. Available from: doi: 10.3892/mco.2016.872.

52. BROUWER, C. L., et al. CT-based delineation of organs at risk in the head and neck region: DAHANCA, EORTC, GORTEC, HKNPCSG, NCIC CTG, NCRI, NRG Oncology and TROG consensus guidelines. *Radiotherapy and oncology: journal of the European Society for Therapeutic Radiology and Oncology* [online]. 2015, **117**(1), 83–90 [viewed 17 March 2023]. Available from: doi: 10.1016/j.radonc.2015.07.041.
53. GONDI, V., et al. Preservation of memory with conformal avoidance of the hippocampal neural stem-cell compartment during whole-brain radiotherapy for brain metastases (RTOG 0933): a phase II multi-institutional trial. *Journal of clinical oncology: official journal of the American Society of Clinical Oncology* [online]. 2014, **32**(34), 3810–3816 [viewed 17 March 2023]. Available from: doi: 10.1200/JCO.2014.57.2909.
54. YUEN, A. H. L., et al. Volumetric modulated arc therapy (VMAT) for hippocampal-avoidance whole brain radiation therapy: planning comparison with Dual-arc and Split-arc partial-field techniques. *Radiation oncology* [online]. 2020, **15**(42) [viewed 17 March 2023]. Available from: doi: 10.1186/s13014-020-01488-5.
55. NANGIA, S., et al. The Hippocampus: A New Organ at Risk for Postoperative Radiation Therapy for Bucco-alveolar Cancer? A Dosimetric and Biological Analysis. *Advances in radiation oncology* [online]. 2021, **6**(3), 100681 [viewed 17 March 2023]. Available from: doi: 10.1016/j.adro.2021.100681
56. VERHAEGEN, F. and J. SEUNTJENS. Monte Carlo modelling of external radiotherapy photon beams. *Physics in Medicine and Biology* [online]. 2013, **48**(21), 107-164 [viewed 17 March 2023]. Available from: doi: 10.1088/0031-9155/48/21/r01.
57. EFENDI, M., et al. Monte Carlo Simulation of 6 MV Flattening Filter Free Photon Beam of True Beam STx LINAC at Songklanagarind Hospital. *Sains Malaysiana* [online]. 2017, **46**(9), 1407-1411[viewed 17 March 2023]. Available from: doi: 10.17576/jsm-2017-4609-08.
58. HERSCHTAL, A., et al. Calculating geometrical margins for hypofractionated radiotherapy. *Physics in medicine and biology* [online]. 2013, **58**(2), 319–333 [viewed 17 March 2023]. Available from: doi: 10.1088/0031-9155/58/2/319.
59. FJÆRA, L. F., et al. Spatial Agreement of Brainstem Dose Distributions Depending on Biological Model in Proton Therapy for Pediatric Brain Tumors. *Advances in radiation oncology* [online]. 2020, **6**(1), 100551 [viewed 17 March 2023]. Available from: doi: 10.1016/j.adro.2020.08.008.
60. MCKENZIE, A., M. VAN HERK, and B. MIJNHEER. Margins for geometric uncertainty around organs at risk in radiotherapy. *Radiotherapy and oncology: journal of the European Society for Therapeutic Radiology and Oncology* [online]. 2002, **62**(3), 299–307 [viewed 17 March 2023]. Available from: doi: 10.1016/s0167-8140(02)00015-4.
61. LI, J., et al. Geometric Changes to the Central Nervous System Organs at Risk During Chemoradiotherapy for Locally Advanced Nasopharyngeal Carcinoma. *Journal of Surgery and Research* [online]. 2022, **5**(August), 477-485 [viewed 20 March 2023]. Available from: doi: 10.26502/jsr.10020247.
62. BREEN, S. L., et al. Spinal cord planning risk volumes for intensity-modulated radiation therapy of head-and-neck cancer. *International journal of radiation oncology, biology, physics* [online]. 2006, **64**(1), 321–325 [viewed 20 March 2023]. Available from: doi: 10.1016/j.ijrobp.2005.08.038.

63. PIOTROWSKI, T., et al. Estimation of the planning organ at risk volume for the lenses during radiation therapy for nasal cavity and paranasal sinus cancer. *Journal of medical imaging and radiation oncology* [online]. 2015, **59**(6), 743–750 [viewed 20 March 2023]. Available from: doi: 10.1111/1754-9485.12344.
64. FOURATI, N., et al. PRV brainstem during the nasopharyngeal IMRT: margin calculation and dosimetric implications. *Radiotherapy and Oncology* [online]. 2019, **133**(April), S1020 [viewed 20 March 2023]. Available from: doi: 10.1016/S0167-8140(19)32298-4.
65. ZHANG, S., et al. Analysis of setup error based on CTVision for nasopharyngeal carcinoma during IGRT. *Journal of applied clinical medical physics* [online]. 2016, **17**(4), 15–24 [viewed 20 March 2023]. Available from: doi: 10.1120/jacmp.v17i4.6083.
66. SUZUKI, M., et al. Analysis of interfractional set-up errors and intrafractional organ motions during IMRT for head and neck tumors to define an appropriate planning target volume (PTV)- and planning organs at risk volume (PRV)-margins. *Radiotherapy and oncology: journal of the European Society for Therapeutic Radiology and Oncology* [online]. 2006, **78**(3), 283–290 [viewed 20 March 2023]. Available from: doi: 10.1016/j.radonc.2006.03.006.
67. MONGIOJ, V., et al. Set-up errors analyses in IMRT treatments for nasopharyngeal carcinoma to evaluate time trends, PTV and PRV margins. *Acta Oncologica* [online]. 2011, **50**(1), 61-71, 2011[viewed 20 March 2023]. Available from: doi:10.3109/0284186X.2010.509108.
68. KOIVUMÄKI, T., et al. Geometrical uncertainty of heart position in deep-inspiration breath-hold radiotherapy of left-sided breast cancer patients. *Acta oncologica* [online]. 2017, **56**(6), 879–883 [viewed 20 March 2023]. Available from: doi: 10.1080/0284186X.2017.1298836.
69. PARK, E. T., and S. K. PARK. Setup uncertainties for inter-fractional head and neck cancer in radiotherapy. *Oncotarget* [online]. 2016, **7**(29), 46662–46667 [viewed 20 March 2023]. Available from: doi: 10.18632/oncotarget.9748.
70. CHANG, J. et al. Positional Accuracy of Treating Multiple Versus Single Vertebral Metastases with Stereotactic Body Radiotherapy. *Technology in Cancer Research & Treatment* [online]. 2017, **16**(2), 231-237 [viewed 20 March 2023]. Available from: doi:10.1177/1533034616681674.
71. LAAKSOMAA, M., et al. AlignRT® and Catalyst™ in whole-breast radiotherapy with DIBH: Is IGRT still needed? *Journal of applied clinical medical physics* [online]. 2019, **20**(3), 97–104 [viewed 20 March 2023]. Available from: doi: 10.1002/acm2.12553.
72. LI, D., et al. Study of Spinal Cord Substructure Expansion Margin in Esophageal Cancer. *Technology in Cancer Research & Treatment* [online]. 2021, **20**(June) [viewed 20 March 2023]. Available from: doi: 10.1177/15330338211024559
73. VAN HERK, M. Errors and margins in radiotherapy. *Seminars in radiation oncology* [online]. 2004, **14**(1), 52–64 [viewed 24 April 2023]. Available from: doi:10.1053/j.semradonc.2003.10.003.
74. MANDAL, A. et al. Set-up Errors and Determination of Planning Target Volume Margins Protocol for Different Anatomical Sites in a Newly Established Tertiary Radiotherapy Centre in India. *Asian Journal of Oncology* [online]. 2020, **6**(02), 81-87 [viewed 10 May 2023]. Available from: doi: 10.1055/s-0040-1710146.
75. INFUSINO, E. et al. Estimation of patient setup uncertainty using BrainLAB Exatrac X-Ray 6D system in image-guided radiotherapy. *Journal of applied clinical medical physics* [online]. 2015, **16**(2), 5102 [viewed 10 May 2023]. Available from: doi: 10.1120/jacmp.v16i2.5102.

76. OH, S. A., et al. Analysis of the Setup Uncertainty and Margin of the Daily ExacTrac 6D Image Guide System for Patients with Brain Tumors. *PloS one* [online]. 2016, **11**(3), e0151709 [viewed 10 May 2023]. Available from: doi: 10.1371/journal.pone.0151709.
77. SUZUKI, J., et al. Uncertainty in patient set-up margin analysis in radiation therapy. *Journal of radiation research* [online]. 2012, **53**(4), 615–619 [viewed 10 May 2023]. Available from: doi: 10.1093/jrr/rrs003.
78. FAN, X., et al. Dosimetric analysis of radiation-induced brainstem necrosis for nasopharyngeal carcinoma treated with IMRT. *BMC Cancer* [online]. 2022, **22**(178) [10 May 2023]. Available from: doi: 10.1186/s12885-022-09213-z.
79. MARKS, L. B., et al. Use of normal tissue complication probability models in the clinic. *International journal of radiation oncology, biology, physics* [online]. 2010, **76**(3 Suppl), S10–S19 [viewed 10 May 2023]. Available from: doi: 10.1016/j.ijrobp.2009.07.1754.